Ann. Phys. (Leipzig) **11** (2002) 2, 95–150

Fundamental Physics in Space: A guide to present projects

C. Lämmerzahl[1]* and H. Dittus[2]

[1] Institute for Experimental Physics, Heinrich-Heine University Düsseldorf, 40225 Düsseldorf, Germany
[2] ZARM, University of Bremen, Am Fallturm, 28359 Bremen, Germany

Received 13 July 2001, revised 31 October 2001, accepted 2 November 2001 by F. W. Hehl

Abstract. A review is presented about most of the current Fundamental Physics (FP) projects in space. After illustrating of what is meant by FP and which are its objectives, reasons are expatiated of why it is of great advantage to do FP in space. Then we give extensive introductions into all present and future FP projects in space. This consists of an explanation of the various scientific objectives, a description of the scientific payload and the used technologies, and an outline of the planned mission scenarios. Furthermore, we give a guide to further information (review papers, web-pages) about the various projects.

Keywords: fundamental physics, space missions, tests of Special and General Relativity, Equivalence Principle, gravitational red shift, gravitational waves, gravitomagnetism, Maxwell's equations
PACS: 04.80.−y, 06.30.−k, 91.10.−v, 95.40.+s, 95.55.−n

Contents

* Corresponding author: claus.laemmerzahl@uni-duesseldorf.de

 0003-3804/02/0202-0095 $ 17.50+.50/0

List of Acronyms

ACES	Atomic Clock Ensemble in Space
AOCS	Attitude and Orbit Control
ASTROD	Astrodynamical Space Test of Relativity using Optical Devices
ASU	Atomic Sagnac Unit
ATHENA	AnTi HydrogEN Apparatus (at CERN)
ATOPIS	ATomic OPtics and Interferometry in Space
BEST	Boundary Effects near Superfluid Transitions
FEEP	Field Electrical Emission Propulsion
FP	Fundamental Physics
FPAG	Fundamental Physics Advisory Group of ESA
GG	Galileo Galilei

GGG	Galileo Galilei on the Ground
GP-A	Gravity Probe A
GP-B	Gravity Probe B
HYPER	HYPER precision atomic interferometer in space
ISS	International Space Station
JPL	Jet Propulson Laboratory
LAGEOS	LAser GEOdynamic Satellite
LISA	Laser Interferometer Space Antenna
LLR	Lunar Laser Ranging
LPI	Local Position Invariance
LTMPF	Low Temperature Microgravity Physics Facility (on the ISS)
MAARS	Micron Accuracy Absolute Ranging System
MICROSCOPE	Micro-satellite a traînée Compensée pour l'Observation du Principe d'Équivalence
MOT	Magneto Optical Trap
MWL	MiocroWave Link
ONERA	Office National de Rechèrches et d'Études Aérospatiale
OPTIS	Optical Test of the Isotropy of Space
PHARAO	Projet d'Horloge Atomique par Refroidissement d'Atomes en Orbite
PPARC	Particle Physics and Astronomy Research Council
SEE	Satellite Energy Exchange
SMART	Small Mission for Advanced Research in Technology
SR	Special Relativity
SQUID	Superconducting Quantum Interference Device
STEP	Satellite Test of the Equivalence Principle
STM	SpaceTime Mission
SUE	Superfluid Universality Experiment
SUMO	Superconducting Microwave Oscillator
T2L2	Time Transfer by Laser Link
UFF	Universality of Free Fall
VLBI	Very Long Basalion Interferometry
WEAX	Weak Equivalence Antiproton eXperiment
WEP	Weak Equivalence Principle

1 Introduction

Today the two basic theories of physics, General Relativity and Quantum Theory, are questioned. Both cannot be correct, because it is not possible to quantize General Relativity along the lines given by conventional quantum theory. Though many approaches are under development for attacking this problem, which in most cases deal with modifications of General Relativity, no satisfactory final result has been achieved until now. Nevertheless, all such approaches predict small violations of the present basic physical theories. Therefore it is mandatory to look for possibilities for improving the experimental search for such kinds of deviations. This is connected with an increasing accuracy of experimental setups which can be achieved, however, only under certain circumstances. In many cases these circumstances are realized in a space environment with well defined space conditions and low noise environment. Thus high precision experiments in space become more and more important for testing the basic properties and predictions of fundamental physical theories.

This is also reflected in the fact that more and more fundamental physics missions are proposed and carried through. Because of the increasing importance of fundamental physics in space for the physics community, in this paper a review about the past, current, and future missions is given.

First we define what we mean by Fundamental Phyiscs (FP) and describe to some extend some of the basic experimental searches in FP. By doing so, we also identifiy the need and conditions for performing experiments under space conditions. Then we present all of these fundamental physics projects and describe their scientific objections, their science payload and the mission scenario.

For other accounts of fundamental physics in space one may contact the NASA roadmap [1], the Community Report to PPARC Space Science Advisory Group [122], the review [108], the convenor's summaries of the ESA-CERN workshop held in April 2000 [60], recent proceedings [70], the forthcoming final report of the ESA Topical Team ATOPIS (Atom Optics and Interferometry in Space) [35], and the forthcoming roadmap of the ESA FPAG.

2 What is Fundamental Physics

2.1 Areas of Fundamental Physics

Todays FP consists of two areas: the area of universal theories and the area of interactions. The universal theories are

- Quantum Theory [characterized by $\hbar$]
- Special Relativity [characterized by c]
- General Relativity [characterized by $\kappa = G/c^2$]
- Statistical phyiscs [characterized by k_B]

and the theories dealing with the four interactions

- gravitational interaction [characterized by G]
- electromagnetic interaction [characterized by α]
- weak interaction [characterized by α_{weak}]
- strong interaction [characterized by α_{strong}]

The *universal theories* are, of course, valid universally and thus have to be applied to all kinds of matter: All matter has to be treated quantum mechanically, all types of matter have to obey the relativity principle and thus must obey, at least locally, the laws of Special Relativity. All kinds of matter act as source for the gravitational field, and all sorts of matter feel the gravitational force, and, as last universal theory, statistical physics or condensed matter physics is a frame theory for many particle systems which extracts from the huge number of degrees of freedom a few experimental accessible quantities.

Consequently, one part of FP is to continue (i) testing the basic foundations and (ii) verifying fundamental predictions of these universal theories, simply because they are the basis of modern physics. These experiments are, e.g., the search for gravitational waves, a test of the Lense-Thirring effect, testing basics of quantum theory, like the linearity of quantum mechanics, measuring with ever increasing precision the values of fundamental constants, like the gravitational constant or the fine structure constant. Such tests are mandatory in order to understand and interpret properly the underlying theories.

As can be seen from the list of interactions, the gravitational interaction plays a double role both as a universal theory and as a particular interaction, which certainly is one reason for the difficulties in quantizing gravity or unifying it with the other interactions (indeed, all attempts in this direction lead to a violation of its universality). While experiments discovering the structure of the electromagnetic interaction are, due to its strength and its range, mainly table-top experiments, the weak and the strong interaction can be accessed only by means of very high energies and can thus be explored mainly with the help of particle accelerators and by observing high energy cosmic rays. However, there are attempts to explore the weak interaction in molecular physics, too. The strong interaction is accessible in space missions through astrophysical observations only, and not by means of experiments with or on satellites.

2.2 Basic problems in Fundamental Physics

There are some basic questions which remained unsolved despite of a huge effort during the last decades: The first and most important problem ist the quantization of gravity. There are several approaches, namely string theory and the canonical quantization of gravity or loop gravity. While the canonical quantization procedure focus on the quantization of gravity, string theory, in addition, also aims to unify all interactions.

Another problem concerns the unification of all interactions. The unified description of the electromagnetic and weak interaction as a $U(1) \times U(2)$ gauge theory has been carried through successfully, and the experimental verification of the present scheme for the unification of these two forces with the strong force is on a good way. Also the detection of the Higgs-boson verifying the mass generation scheme of gauge theories seems to be a matter of time only. The unification of these interactions with gravity was attacked by means of gauge theory, Klein-Kaluza theory, supergravity and string theory and its variants. The most appealing approach today is M-theory, a theory behind the various string theories.

A good reason in favour of the unification procedure are the universality principles of Special and General Relativity, namely the relativity principle, the Weak Equivalence Principle and the universality of the gravitational red shift. While these universality principles play an important role as a guiding principle for inventing new theories, they are of course an idealization of physical *experience* and should follow from that. The main point of the relativity principle, for example, is the statement that for all kinds of matter the maximum propagation speed (in vacuum) is the speed of light. Since all particles, neutrons, electrons, photons, gravitons, etc, “know” the same maximum speed, that is, since all these *different* particles share *common properties*, one may conclude that they must have some common origin. Analogously, since all non-gravitational physics, that is, all kinds of interactions, behave locally in the same way in a gravitational field, all these interactions again must have some origin in common. Therefore a unification of all interactions appears to be a reasonable scheme behind the phenomena of physics.

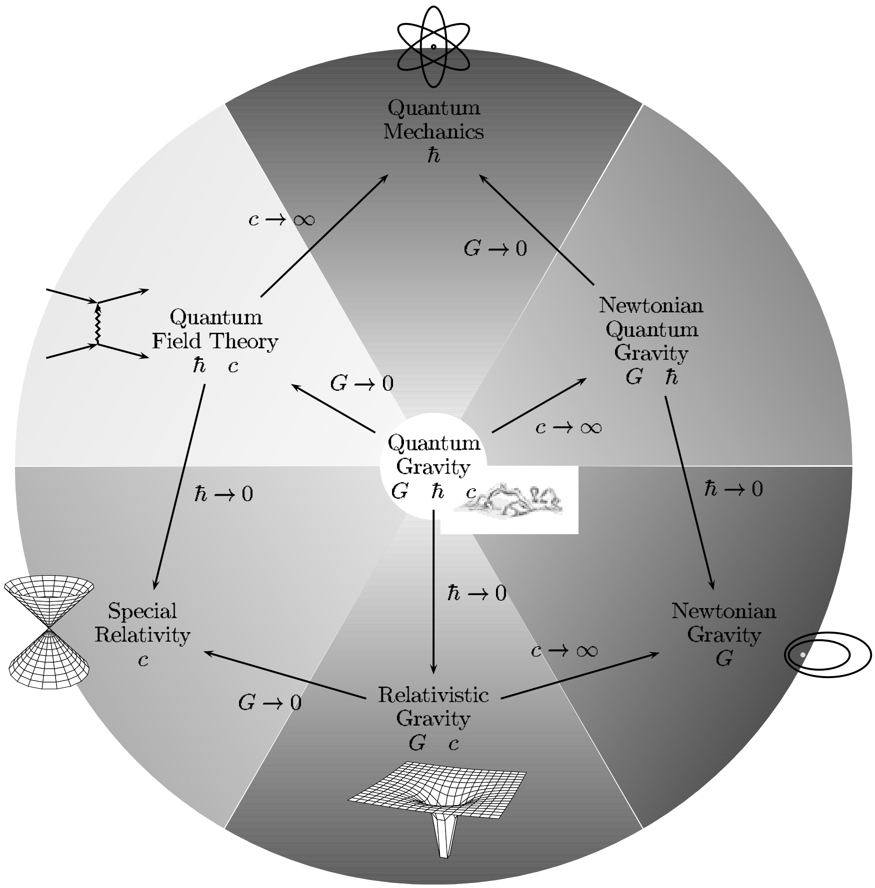

Fig. 1 The magic circle of Fundamental Physics: Structure and interdependence, in view of a quantum gravity theory, of the three universally applicable theories Quantum Theory, Special Relativity and Gravity (General Relativity).

However, all aproaches to a quantum gravity theory and also the approaches aiming to unify all interactions, in general lead to deviations from present day physics by violating the universality principles. For reasons of theoretical consistency, one would have to introduce additional interactions in the form of additional scalar fields which couple differently to different kinds of elementary particles and thus violate the Equivalence Principle and the universality of the gravitational red shift. There also appear Yukawa-like gravitational forces introducing a mass of the graviton, which also may depend on matter. A time-dependence of fundamental constants is also a scenario favoured by the unification scheme. Furthermore,

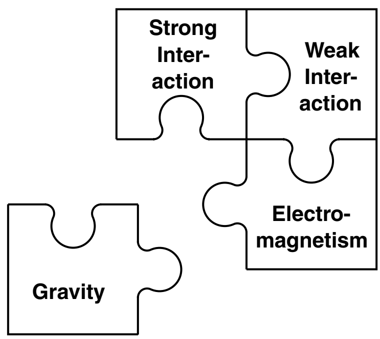

modifications of Maxwell's equations are derived within string theory and loop gravity leading to violations of, e.g., the isotropy of light propagation.

Though this seems to be contradictory to the initial wish of looking for a unified physics, it nevertheless gives the direction for an experimental search for possible measurable effects as predicted by the unification schemes: Violation of the Equivalence Principle or of the universality of the gravitational red shift, Yukawa-parts of the gravitational interaction, additional gravitational interaction with the spin of particles, search for a time-dependence of the gravitational constant or of the fine structure constant, search of deviations from Maxwell's equations, etc.

3 Questions in Fundamental Physics

In this section, we want to present some general issues which may be worth to be considered and tested in the future and the results of which may give further insight into physics. Due to lack of space, we leave out issues if cosmology and astrophysics which as well may be considered as part of fundamental physics.

3.1 Quantum Theory

Principles of Quantum Mechanics

- Superposition principle
- Uncertainty

What the Equivalence Principle is for General Relativity, is the Superposition Principle for Quantum Mechanics. The Superposition Principle describes the wave nature of matter which is the main feature of Quantum Mechanics. Therefore, as for the Equivalence Principle, it is mandatory to test the Superposition Principle with ever-increasing precision, which is one of the points we will mention below.

Since Quantum Mechanics is the physics on a small spatial scale, in most cases, as in spectroscopy, for example, also only small timescales are involved. However, due to the tremendous progress in the precise manipulation of single quantum systems, like laser cooling, it is nowadays possible to prepare and isolate quantum systems with very low velocities of the order of mm/s. These quantum systems may have a lifetime of many seconds or even longer so that it should be possible in principle to perform interference experiments, for example, where the coherently split wave functions remain separated for seconds or even longer before they recombine again. However, this is possible only if the wave functions do not fall outside of the interferometer. Therefore it is necessary to carry out experiments under weightlessness conditions in order to use the advantage of a long free evolution time which has the potential to increase enormously the experimental accuracy.

Among a lot of issues in quantum mechanics, there are some which may be possible candidates for space experiments.

Decoherence Long free evolution times are important for studies of the decoherence of quantum systems which can be described by a non-unitary part of the Hamilton-operator $H = H_0 + i\alpha$, with the usual hermitian Hamiltonian H_0 and an hermitian operator α. The question whether quantum systems suffer decoherence in vacuum may be observable with interferometry by searching for a decrease of the visibility of interference fringes as function of the free evolution before recombination of the coherently split wave function. The longer the free evolution time is, the better the sensitivity for this kind of phenomena. There are hypotheses that decoherence is a quantum gravity effect due to quantum gravity induced fluctuations of space-time [32, 91].

Linearity of Quantum Mechanics The property of quantum systems to show interference is one of the miracles of physics which, however, is confirmed by many observations. A hypothetical non-linear quantum mechanics, which, under certain circumstances, can be described by a Hamiltonian $H = H_0 + \alpha \ln (a\,|\psi|^2)$ with a real α [115], again is a feature which can best be tested by means of interferometry. With neutron interferometry, nonlinearities have been excluded with $\alpha \leq 3.4 \cdot 10^{-13}$ eV [116]. A considerable improvement of this result is conceivable by means of atom interferometry in space using the advantage of a long free evolution time.

Entanglement/correlations Another distinguished feature of quantum mechanics is the entanglement of states. This is connected with a non-local behaviour of quantum systems. Many features of quantum theory, like quantum teleportation, Einstein-Podolski-Rosen paradoxa, Greenberger-Horne-Zeilinger states, quantum computing, etc. are connected with entanglement, see [9, 12] for reviews.

Measurement process The understanding of the measurement process is one of the unsolved problems in quantum mechanics. In the conventional interpretation of quantum mechanics, it is described by the postulate of the reduction of the wave function. This seems to be contradictory if the physical system under consideration *and* the measurement apparatus (which should be part of the physical world) both are described quantum mechanically. Solutions to that problems are, e.g., a many-world-interpretation of Quantum Mechanics or the decoherence of the physical state under consideration through its interaction with the measurement apparatus so that the final state of the physical systems effectively (after the measurement process) looks like a reduction of the wave packet had taken place. There are speculations where the reduction is ascribed to a fundamental decoherence or to a modified dynamics for large systems, see [16, 63] for a survey of this issue.

Casimir effect The Casimir effect is a macroscopic effect which can be explained only by means of second quantization of the Maxwell field describing the creation and annihilation of photons. The main consequence of second quantization is the prediction of vacuum fluctuations. These fluctuations depend on the physical boundary conditions. They are different for free space compared with a restricted region of space only. This difference leads to the famous Casimir effect: The difference in the energy of the vacuum fluctuation between nearby condensator plates and widely separated plates leads to a distance-dependent force between neutral

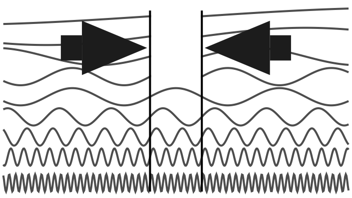

Fig. 2 The Casimir effect: owing to the boundary conditions there are more electromagnetic waves (modes) outside two conducting parallel plates than inside leading to a quantum pressure on the plates from outside.

condensator plates, see Fig. 2. This effect has been verified in experiments [73, 102]. It is desirable to improve the accuracy of the experiments, because of the fundamental importance of this effect, and to explore further related effects, e.g. [42].

Bose-Einstein condensation If identical bosonic quantum systems are cooled down to very low temperatures (of the order of nK), then the wavefunctions of the individual systems overlap and the whole system begins to become one single giant quantum state, the Bose-Einstein condensate. In this condensate all atoms are coherently linked. This leads to new phenomena which have important applications in interferometry and metrology. For example, Bose-Einstein condensates may be the source for a coherent atomic beam thus serving as an atom laser. A use of these coherent atomic beams in atom interferometers will increase the sensitivity of these devices by orders of magnitude and can furthermore be used for a more precise determination of fundamental constants as, e.g., the fine structure constant. Other issues in the quantum domain are concerned with the coupling of quantum matter to external fields, in particular the coupling to inertial and gravitational fields, and the coupling of the elementary particle spin to these fields. We will consider these questions in the gravity section.

3.2 Special Relativity

Principles of Special Relativity

- Constancy of speed of light
- Relativity principle

The main ingredient of Special Relativity is the relativity principle which has the status of a universality principle. It states that there is no single physical phenomenon which singles out a distinguished inertial frame of reference. In the words of a universality principle: *all* phenomena happen in the same way in *all* inertial frames. If in two inertial frames we have the same initial and boundary conditions with respect to the corresponding coordinate systems, then the dynamics of the physical systems is identical in both inertial frames. This includes the fact that all particles possess as maximum speed the velocity of light: a different maximum speed of one particle would single out a preferred frame thus violating the relativity principle. Correspondingly, all tests of Special Relativity are mainly tests of the relativity principle.

In the following, c is the characteristic velocity (in the sense of a limiting velocity, for massive particles) of *all* kinds of particles, not only of photons. Tests of Special Relativity are usually described within the *kinematical* test theories of Robertson [101] or Mansouri and Sexl [78–80] replacing the old ether "test"-theory by a theory allowing parametrized deviations from Lorentz-transformations. In Special Relativity the propagation of light is described by $0 = \mathrm{d}s^2 = c^2\,\mathrm{d}t^2 - \mathrm{d}\boldsymbol{x}^2$ which is equivalent to the constancy of $c^2 = \mathrm{d}\boldsymbol{x}^2/\mathrm{d}t^2$. Since all coordinates appear in the same way, no preferred inertial frame can be singled out.

This symmetry is broken if one assumes that light propagates according to $0 = \mathrm{d}s^2 = g_0^2(v)\,c^2\,\mathrm{d}t^2 - \left(g_1^2(v)\,\mathrm{d}\boldsymbol{x}_\parallel + g_2^2(v)\,\mathrm{d}\boldsymbol{x}_\perp\right)$, where v is the velocity with respect to the preferred frame where light propagates isotropically and where $\boldsymbol{x}_\parallel$ and $\boldsymbol{x}_\perp$ are the components of the spatial coordinates parallel and orthogonal to the velocity $\boldsymbol{v}$. Since in this model $g_0(0) = 1$, $g_1(0) = 1$, and $g_2(0) = 1$, violations of Special Relativity are of purely kinematical origin.

Then, for non-vanishing velocity $\boldsymbol{v}$, the velocity of light is given by

$$c(v, \vartheta) = \frac{c g_0(v)}{\sqrt{g_2^2(v) - (g_2^2(v) - g_1^2(v)) \cos^2 \vartheta}}\,, \tag{1}$$

where ϑ is the angle between the velocity of the moving frame and the direction of light propagation and where c is the velocity of light in the preferred frame. If we expand $g_i(v) = 1 + g_i^0 v^2/c^2 + \ldots$, $i = 0, 1, 2$, then we get

$$c(v, \vartheta) = c\left(1 + A\,\frac{v^2}{c^2}\sin^2\vartheta + B\,\frac{v^2}{c^2} + \mathcal{O}(v^4/c^4)\right), \tag{2}$$

with $A = g_1^0 - g_2^0$ and $B = g_0^0 - g_1^0$. Obviously, the equality of g_1 and g_2 ensures the isotropy of the speed of light, and the equality of g_0 and g_1 states that the speed of light does not depend on the velocity of the chosen frame. Finally, the time dilation factor $g_0(v)$ has to be determined by e.g. Doppler-shift experiments.

Owing to a different approach, in the Mansouri-Sexl test theory other parameters are used:

$$A \to \tfrac{1}{2} - \beta + \delta\,, \qquad B \to \beta - \alpha - 1\,. \tag{3}$$

Special Relativity is uniquely characterized by $g_0(v) = g_1(v) = g_2(v) = 1$. To second order, this means $g_0^0 = g_1^0 = g_2^0 = 0$ or $\alpha = -\frac{1}{2}$, $\beta = \frac{1}{2}$, and $\delta = 0$. According to the analysis of Robertson [101], Special Relativity can be completely determined from tests on the isotropy of light propagation (Michelson-Morley experiments), on the independence of the velocity of light from the velocity of the laboratory (Kennedy-Thorndike experiments), and on time dilation experiments (Ives-Stilwell experiments). Note that according to the relativity principle, c has the meaning of the velocity of light or the limiting velocity of massive particles.

Despite of the very successful Robertson-Mansouri-Sexl test theory, it is clear that there is no single unique test theory. There are other frames for the consistent description of tests of Special Relativity, each emphasizing other important aspects of Special Relativity. In many cases, they have to be explored in different experiments.

Within a *dynamical* test theory, an anisotropic propagation of light is connected with a so-called constitutive tensor χ^{abcd} emerging in the 'kinetic' part of the generalized Maxwell equations,

$$4\pi j^a = \chi^{abcd}\,\partial_b F_{cd} + \chi^{abc} F_{bc}\,. \tag{4}$$

This has not the form as given by Special Relativity, namely $\chi^{abcd} = \eta^{a[c}\eta^{d]b}$, where η^{ab} is the space-time metric. For quantum matter, the dynamical realization of an anisotropic limiting velocity is given by a generalized Dirac equation

$$0 = i\gamma^a\,\partial_a\psi + M\psi\,, \tag{5}$$

where the matrices γ^a fail to form a Clifford algebra [67]. Such generalized field equations for the electromagnetic field and for the field of a spin-$\frac{1}{2}$-particle are predicted by quantum gravity [2, 33, 34, 44]. In the non-relativistic limit of the generalized Dirac equation, there appear anomalous inertial mass tensors which violate Special Relativity and lead to a splitting of Zeeman-singlet lines which are searched for in nuclear spectroscopy (Hughes-Drever experiments, [21, 31, 62, 74, 94]).

Even if both equations, the generalized Maxwell as well as the generalized Dirac equation, reduce to their respective Special Relativistic form, then it is still an open question whether the maximum speed of the Dirac particles is the same as the velocity of light. This question is addressed in the so-called $TH\epsilon\mu$-formalism [124, 131]. As a result of this test theory, there are again anomalous inertial mass tensors in the effective field equation for atoms in a moving frame which are experimentally accessible by Hughes-Drever experiments.

Isotropy of c The isotropy of the maximum velocity of particles like photons, electron, etc. have been and can be tested with different methods. The isotropy of the speed of photons can be tested with a Michelson-Morley interferometer or with corresponding tests using microwave or optical cavities [10]. A hypothetical non-isotropy of the maximum velocity of massive particles will become manifest in an anisotropic anomalous inertial mass tensor which, if we have particles with spin, may also depend on the spin of the particle under consideration. Such anomalous inertial mass tensors can be searched for by means of Hughes-Drever experiments [67]. These are spectroscopic experiments which look for a splitting of the single Zeeman-line in electronic or nuclear energy levels.

It should be noted that Michelson-Morley experiments are not only sensitive to an anisotropic speed of light but also to the physics of the interferometer arms or of the cavity: Indeed, if light propagates anisotropically, then this must have its origin in modified Maxwell equations. Due to the complicated and interlinked structure of the Maxwell equations, this kind of modification also influences the electrostatic potential of electric charges. Since just this potential is crucial for the properties of solids, it is clear that also the interferometer arms and the cavity are influenced in a general material dependent way. For a certain model, this has been calculated [71]. As a historical note we mention that already Morley and Miller searched for a material dependent FitzGerald-Lorentz contraction in their experiments [82, 83].

Independence of c from the velocity of the source If Special Relativity is valid, then the velocity of the photon or the limiting velocity of massive particles does not depend on the velocity of the corresponding source. This statement can also be interpreted as a special case of the Einstein velocity addition theorem.

For light this principle can be tested in the same way as the isotropy of space: By means of interferometry, which amounts to a Kennedy-Thorndike experiment [64], or with cavities, as has been used by Hils and Hall [55]. As far as direct tests of the limiting velocity of particles are concerned, until now no experiments have been carried through.

These experiments can again be described within the Robertson and Mansouri-Sexl kinematic test theory. Also within the frame of the modified Maxwell equation a change in the reference frame leads to velocity dependent effects. In both cases, the dependence of the velocity of light from the velocity of the laboratorys frame can be expressed as $c(v) = c + \kappa v^2/c^2$. Therefore, it becomes clear that the larger the change in the velocity is, the better one can give estimates on κ. Furthermore, this kind of experiment clearly calls for being performed in space where changes in the velocity can be one order of magnitude larger than on Earth.

Doppler effect With the Doppler effect one measures the time dilation factor which in Special Relativity acquires the form $1/\sqrt{1 - v^2/c^2}$, where v is the relative velocity between sender and observer. The accuracy of corresponding tests increases with larger velocities and with sharper absorption lines. However, in ion accelerators [48], for example, much higher velocities can be obtained than with satellites, and for the Mössbauer rotor experiments the velocity needs not to be such large because the Mössbauer line is very sharp.

3.3 General Relativity and gravitation

Principles of General Relativity

- Weak Equivalence Principle
- Universality of red shift
- Locally Special Relativity
- Strong Equivalence Principle

Here we address two points: (i) To explore the structure of the coupling of classical and quantum matter with the gravitational field, that is, to explore the form of the gravitational fields and whether there are more than one quantity which may be identified with the gravitational field. In Einsteins GR, there is one quantity, namely the metric $g_{\mu\nu}$ which serves as gravitational field. In other theories torsion may appear, for example, as an additional gravitational field. (ii) To verify predictions of General Relativity experimentally, that is, to explore the structure of the gravitational field equations. For doing so, the dynamics of test particles, that is, small particles with its own gravitational field neglected, play a central role: They are used to explore the structure of the gravitational field (which results in the formulation of the Equivalence Principle) and to determine the gravitational field created by massive sources.

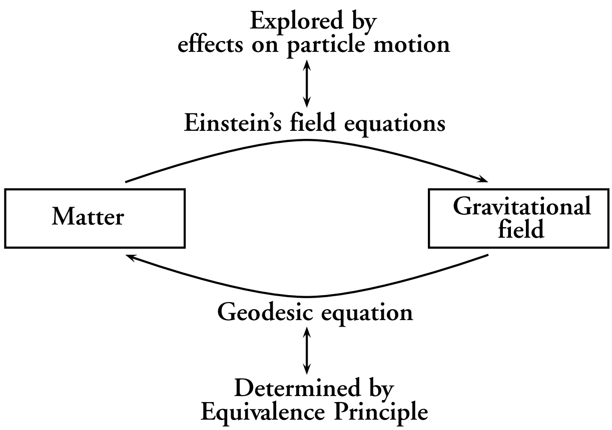

3.3.1 Exploring the structure of the coupling to gravity

The structure of a metric theory of gravity is encoded in the Einstein Equivalence Principle. This principle consists of three parts: (i) all structureless point particles fall along the same path (Universality of Free Fall, UFF), (ii) Special Relativity is valid for small space-time regions, and (iii) physics does not depend on the position in the gravitational field (Local Position Invariance, LPI). The first point is the Weak Equivalence Principle (WEP), the last implies a universality of the gravitational red shift, see below. Consequently, any search for a violation of the WEP, of SR, or of LPI is tantamount to a search for deviations from Einstein's General Relativity as they are predicted from quantum gravity, for example.

The Weak Equivalence Principle The basic principle of Newtonian gravity and General Relativity, proven with very high precision, is the WEP. It states that all kinds of structureless matter fall in a gravitational field along the same path. The main consequence of this principle is the geometrization of the gravitational interaction: Since gravity acts in the same way on all kinds of particles, it can be interpreted as a guiding field, thus defining a space-time geometry.

In experiments, the quantity which represents the validity of the WEP is the Eötvös parameter $\eta_{(1)\,(2)} = 2(a_{(1)} - a_{(2)})/(a_{(1)} + a_{(2)})$ where $a_{(1)}$ and $a_{(2)}$ are the accelerations of two particles measured in a frame in which the gravitating body is at rest. In terms of the usual approach of the inertial and gravitational mass m_i and m_g, $\boldsymbol{F} = m_i \boldsymbol{a} = m_g \boldsymbol{\nabla} U$, where U is the Newtonian gravitational potential, the Eötvös parameter is given by the normalized difference of the ratios of the gravitational and inertial masses for two different particles,

$$\eta_{(1)\,(2)} = 2\,\frac{\mu_1 - \mu_2}{\mu_1 + \mu_2} \quad \text{with} \quad \mu_{1,2} := \frac{m_{\mathrm{g}(1,2)}}{m_{\mathrm{i}(1,2)}}\,, \tag{6}$$

see also [61]. A violation of the WEP at an order of $\eta = 10^{-18}$ to 10^{-15} is predicted in the low energy limit of string theory [26, 27].

For a more general discussion of the WEP, which also addresses Schiff's conjecture, we refer to the approach of Haugan [52, 131]. In this formalism the dynamics of a particle with internal structure is described by means of a general Hamiltonian

$$H = \frac{1}{2m}\left(\delta^{ij} + \frac{\delta m_{\mathrm{i}}^{ij}}{m}\right) p_i p_j + \left(m\delta_{ij} + \delta m_{\mathrm{g}ij}\right) U^{ij}\,, \tag{7}$$

where $\delta m_{\mathrm{i}}^{ij}$ and $\delta m_{\mathrm{g}ij}$ are the anomalous inertial and gravitational mass tensors of the particle, respectively. U is the Newtonian potential, and $U^{ij} = G \int \rho(x')\,(x - x')^i\,(x - x')^j / |x - x'|\,\mathrm{d}^3x'$ is the Newtonian tensor potential. These anomalous mass tensors depend on the form of matter, that is, on the atomic state, for example. From this Hamiltonian it is clear that the ratio of atomic transitions in two different atoms or between different pairs of atomic states of the same kind of atoms (which both constitute two different clocks) depend on the velocity and on the position in the gravitational field:

$$\frac{\nu_1}{\nu_2} = \frac{\Delta E_1^0}{\Delta E_2^0}\left[1 - \frac{1}{2}\left(\frac{\Delta\delta m_{\mathrm{i}1}^{ij}}{\Delta E_1^0} - \frac{\Delta\delta m_{\mathrm{i}2}^{ij}}{\Delta E_2^0}\right)\frac{v^i v^j}{c^2} + \left(\frac{\Delta\delta m_{\mathrm{g}1}^{ij}}{\Delta E_1^0} - \frac{\Delta\delta m_{\mathrm{g}2}^{ij}}{\Delta E_2^0}\right)\frac{U^{ij}(\boldsymbol{x})}{c^2}\right] \tag{8}$$

where $\Delta E^0_{1,2}$ are the energy differences for atoms at rest and in a vanishing gravitational potential. Consequently, anomalous inertial mass tensors are responsible for a frame dependent rate of clocks, thus breaking locally Lorentz invariance, and anomalous gravitational mass tensors are responsible for a position dependent rate of clocks, thus breaking the position invariance of physical processes.

From Eq. (7) we also may derive the acceleration

$$a^i = \left(\delta^{ij} + \frac{\delta m_{\rm i}^{ij}}{m}\right) \partial_j U + \frac{\delta m_{\rm g}\, jk}{m}\, \partial_i U^{jk} \,. \tag{9}$$

Since the anomalous mass tensors in general depend on the chosen material and especially on the atomic state, the WEP (the universality of free fall) is clearly violated. In addition, a violation of local Lorentz invariance or local position invariance leads to a violation of the WEP. Thus, a test of the WEP also amounts to a search for violations of Lorentz invariance and position invariance.

Ordinary matter: In terms of the Eötvös parameter, the WEP has been verified with 10^{-12} accuracy for ordinary matter [121] by using a torsion pendulum.
The precision is mainly limited by the properties of the torsion fibre [18]. Since the almost optimum setup has already been chosen, only small improvements can be expected in the future by using this technique. Also free-fall experiments on Earth in, e.g., drop towers also have a potentiality of 10^{-13} only. A big step in the accuracy will be gained by going into space and by observing the free fall of bodies for a long time; see the proposals MICROSCOPE (p. 126), STEP (p. 133), and GG (p. 142) which aim at a test of the WEP to a precision of 10^{-15}, 10^{-18}, and 10^{-17}, respectively.

Charged matter: Much worse results are obtained for tests with charged matter [134] which were carried out originally as precursor experiments for later tests of the WEP for antiparticles and which are in accordance with the WEP within 10% only. The problems of this experiment are the interaction of the gravitational field with the electromagnetical shielding body [28]: First, the Schiff-Barnhill effect induces an electric field inside the shielding metal which, for an electron, just cancels the gravitational force, and second, the so-called DMRT field which comes from the nonuniform deformation of the metallic lattice in the gravitational field and which induces much more disturbances than the Schiff-Barnhill effect. These disturbances can be avoided by doing the corresponding experiment in space.

As other experimental setups for testing the WEP for charged matter one may use charged particle interferometry or a charged ion in a trap which motion indicates the validity of the WEP for charged particles [V. Lagomarsino, V. Lia, G. Manuzio, and G. Testara, Using a Penning trap to weight antiprotons. Phys. Rev. A **50**, 977 (1994)].

Polarized matter: There are some experiments which look for a violation of the WEP for polarized matter (matter with spin). Speculations about the violation of the discrete symmetries P, C, and T in gravitational fields lead to the following possible interactions involving the spin of the participating bodies, see [75],

$$V(r) = U(r)\,[1 + A_1(\boldsymbol{\sigma}_1 \pm \boldsymbol{\sigma}_2)\cdot\hat{\boldsymbol{r}} + A_2(\boldsymbol{\sigma}_1 \times \boldsymbol{\sigma}_2)\cdot\hat{\boldsymbol{r}}]\,, \tag{10}$$

where $\boldsymbol{\sigma}_{1,2}$ are the spins and $\boldsymbol{r}$ is the distance between the two bodies, $\hat{\boldsymbol{r}}$ is the corresponding unit vector, and $U(r)$ the Newtonian potential. In the case that one body (for example the Earth) is unpolarized, then

$$V(r) = U(r)\,(1 + A\boldsymbol{\sigma}\cdot\hat{\boldsymbol{r}})\,. \tag{11}$$

From hyperfine splittings of the hydrogen ground state, we have $A \leq 10^{-11}$ for protons and $A \leq 10^{-7}$ for electrons, [75].

In [50, 51], the ansatz above is generalized to involve the velocity of the particles,

$$V(r) = U_0(r)\left[1 + A_1\boldsymbol{\sigma}\cdot\hat{\boldsymbol{r}} + A_2\boldsymbol{\sigma}\cdot\frac{\boldsymbol{v}}{c} + A_3\hat{\boldsymbol{r}}\cdot\left(\boldsymbol{\sigma}\times\frac{\boldsymbol{v}}{c}\right)\right], \tag{12}$$

which is still *CPT*-invariant. Here $\boldsymbol{\sigma}\cdot\boldsymbol{r}$ violates P and T, $\boldsymbol{\sigma}\cdot\boldsymbol{v}$ violates P and C, and $\boldsymbol{r}\cdot(\boldsymbol{\sigma}\times\boldsymbol{v})$ violates C and T, see also the note of [92].

In a first type of experiment one searched for polarization dependent *forces* [57, 100], in a second type for an anomalous coupling of spin to external fields on the level of the Hamiltonian [20, 126, 133].

In this context it is appropriate to use quantum matter like neutrons or atoms with a net spin. The most general interaction for particles with rest mass and spin in the nonrelativistic limit is given by [67]

$$\begin{aligned} H = &-\frac{\hbar^2}{2m}\left(\delta^{ij} + \frac{\delta m_{\rm i}^{ij} + \delta\bar{m}_{{\rm i}k}^{ij}\sigma^k}{m}\right)\partial_i\partial_j + \left(\Lambda_j^i + \frac{1}{m}\,\lambda_j^i\right)\sigma^j\partial_i \\ &+ m\left(\delta_{ij} + \frac{\delta m_{{\rm g}ij}}{m} + \frac{\delta m_{{\rm g}k}}{m}\,\delta_{ij}\sigma^k\right)U^{ij} + cT_i\sigma^i + mc^2 B_i\sigma^i\,, \end{aligned} \tag{13}$$

where $\delta m_{\rm i}^{ij}$ and $\delta\bar{m}_{{\rm i}k}^{ij}$ are anomalous inertial mass tensors which may depend on the spin, Λ_j^i and λ_j^i are spin-momentum couplings of different dimensions, $\delta m_{{\rm g}ij}$ is the ordinary anomalous gravitational mass tensor and $\delta m_{{\rm g}k}$ its spin-dependent companion, T_i may be regarded as the vectorial part of an axial torsion coupled to the fully relativistic Dirac equation, and B_i is an additional spin-dependent mass term.

For a search for these anomalous quantities it is certainly of big advantage to have long interaction times and high energies, and to be able to use pure quantum matter. For the latter the spin per mass unit is certainly better than for polarized bulk matter.

Antimatter: The question whether antimatter respects the WEP like ordinary matter is a very exciting question because on the one hand some theories predict antigravity behaviour for antimatter, but on the other hand the validity of the Equivalence Principle fo antimatter can be derived on very general principles, see [46, 87] for reviews on that topic. Since it is very difficult to produce and store a reasonable amount of antimatter, and since tests of the free fall of charged particles are accompanied by huge experimental problems, until now no experiments have been carried out for testing the WEP for antimatter. Nevertheless, space experiments have been proposed recently (WEAX, p. 139 and [58, 59]).

A violation of the WEP amounts to a material dependent modification of the gravitational interaction or an additional force. This (still hypothetical) force is called *fifth force*. Consequently, searching for a fifth force is essentially a search for a violation of the WEP. Owing to theoretical reasons, such a fifth (or sixth, or seventh, ...) force in most approaches for a unified or quantum gravity theory appears as additional scalar field, a scalar potential, connected with certain elementary particles. The gradient of this field gives the additional force under consideration, but also may lead to time and position dependent fundamental constants which modify the behaviour of clocks, etc.

Universality of gravitational red shift Also this universality is a phenomenon which connects all other phenomena of physics: It states that an atomic clock, for example, which is determined by the "motion" of the electron in the Coulomb-potential of the nucleus, behaves in the same way as an optical clock, where the "ticks" of the clock are given by the bouncing of a photon at the mirrors at the two end sides of an optical cavity. Another example is that an atomic transition between states given by principal quantum numbers behave in the same way as a hyperfine transition. Though all these clocks are based on two completely different physical processes, they experience the same redshift in a gravitational field. This also applies to all kinds of clocks, to different atomic clocks, for example, which may depend on different atomic transitions, to the H-maser, etc. The essential point is that different clocks depend in a different way on physical constants, on the fine structure constant or on the ratio of the electron to proton mass, for example. Time units based on different physical processes depend differently on various constants and are based on different physical principles. Thus the universality of the gravitational red shift states that these constants are really constant in space and time.

The gravitational red shift is given by

$$\nu(x_1) = \left(1 - \frac{U(x_1) - U(x_0)}{c^2}\right) \nu(x_0)\,, \tag{14}$$

where $U(x)$ is the Newtonian gravitational potential at position x. For a non-universal red shift the frequency difference depends on the used clock

$$\nu(x_1) = \left(1 - (1 + \alpha_{\text{clock}})\,\frac{U(x_1) - U(x_0)}{c^2}\right) \nu(x_0)\,. \tag{15}$$

In standard theory $\alpha_{\text{clock}} = 0$. Therefore, in first order of the potential difference, the ratio of the frequencies of two clocks is given by

$$\frac{\nu_{\text{clock}\,1}(x_1)}{\nu_{\text{clock}\,2}(x_1)} \approx \left(1 - (\alpha_{\text{clock}\,2} - \alpha_{\text{clock}\,1})\,\frac{U(x_1) - U(x_0)}{c^2}\right) \frac{\nu_{\text{clock}\,1}(x_0)}{\nu_{\text{clock}\,2}(x_0)}\,, \tag{16}$$

which is a special case of Eq. (8). Consequently, a common motion of both clocks in a gravitational field yields a signal in the frequency ratio which scales with the potential difference $(U(x_1) - U(x_0))/c^2$. It is obvious that for a good estimate on the anomalous clock parameter α_{clock} the use of high precision clocks and space missions are mandatory, see the missions GP-A (p. 121), PHARAO/ACES (p. 131), SUMO (p. 135), SpaceTime (p. 136), and OPTIS (p. 141).

An interesting aspect of this point may be to test the universality of the gravitational red shift for an "anti-clock", that is, for a clock made from an anti-atom. Since clocks may be based on a single trapped ion, it should be possible to base a clock on a single anti-ion.

Yukawa-force Many unifying and quantum gravity theories predict the existence of an additional Yukawa-like gravitational potential so that the total gravitational potential reads $U = G(M/r)\left(1 + \alpha\, e^{-\lambda r}\right)$, where G is the usual gravitational constant and M the mass of the gravitating body. α and λ are the strength and the range, respectively, of the additional Yukawa potential, compare [40]. Yukawa potentials are also connected with higher dimensional theories, see e.g. [65]. With LLR (Lunar Laser Ranging, see p. 122) this deviation from Newton's $1/r$-potential can be excluded with an accuracy of $\alpha \leq 10^{-12}$ at a range of the order of the Earth-Moon distance. However, most predictions tell that the range of such a Yukawa part should be smaller than a mm. This has been tested down to 218 μm [56] where no deviations from the inverse-square law have been found. Perhaps this is best to be explored with small objects like atoms.

Fundamental constants Due to the above mentioned scalar fields which arise in quantum gravity and unification schemes the gravitational constant G, the fine structure constant $\alpha = e^2/\hbar c$, or the ratio of the proton to the electron mass m_p/m_e may become time and position dependent. No such time or position dependence has been found until now, except a claim for an observation of a cosmological variation of the fine structure constant [130]. This may also be connected with charge conservation, see p. 115.

If the value of the gravitational constant becomes smaller, for example, then this will result in weakening of the gravitational attraction between the moon and the earth, for example, yielding an increasing distance between these two objects. Indeed, using LLR, the time-dependence of G has been restricted to $\dot{G}/G \leq 5 \cdot 10^{-12}\ \mathrm{yr}^{-1}$ [110]. Further missions trying to improve these estimates are ASTROD (p. 138) and SEE (p. 140).

Space-time fluctuations See decoherence, p. 101.

Coupling of quantum fields with inertial and gravitational fields Since quantum fields possess more degrees of freedom than classical particles and are extended objects, they may couple to gravity and inertia in a way different than it is expected from the point of view of classical physics of point particles. Until now no deviation from these expectations are found: gravity and inertial fields act on quantum systems as it is predicted from the minimal coupling procedure. However, owing to their small extension, gravity, in the sense of a coupling of curvature or other geometrical fields, influences quantum systems only very weakly. Nevertheless, quantum systems are very sensitive to acceleration and rotation. Consequently, accelerometers and gyroscopes based on atoms are under construction which will yield better accuracy than similar devices based on lasers (see HYPER, p. 137).

3.3.2 Testing predictions of General Relativity

There are a lot of very important physically most relevant phenomena and aspects of General Relativity, like black holes, cosmology, gravitational lensing etc., which are left out here, because we restrict ourselves to experiments which can be tested and explored in the laboratory and in space, if one makes use of the very advantageous space conditions (see p. 117). That means, we leave out missions like AMS, EUSO, MAP, PLANCK, etc., which explore fundamental physics issues merely by astrophysical observations.

The predictions of GR are most appropriately described within the framework of a Parametrized Post-Newtonian approximation (PPN-formalism) [81, 131]. A simpler special case of this general scheme is the Eddington parametrization with only three parameters α, β, and γ:

$$g_{00} = 1 - \alpha \frac{U}{c^2} + 2\beta \frac{U^2}{c^4} + \mathcal{O}\left(1/c^6, \text{radiation reaction}\right), \tag{17}$$

$$g_{0i} = (1+\gamma) \frac{V_i}{c^3} + \mathcal{O}\left(1/c^5, \text{radiation reaction}\right), \tag{18}$$

$$g_{ij} = -\delta_{ij} \left(1 + 2\gamma \frac{U}{c^2}\right) + \mathcal{O}(1/c^4, \text{radiation reaction}). \tag{19}$$

Here U is the Newtonian potential and $V_i = G \int \frac{\rho(x')\,(x-x')^i}{|x-x'|}\, d^3x'$ (the parameters α and β should not be mixed up with the Mansouri-Sexl parameters or the fine structure constant). The three parameters α, β, and γ parameterize gravitational theories. GR is uniquely characterized by $\alpha = \beta = \gamma = 1$. As above, the parameter α describes the gravitational red shift, the parameter γ describes the value of the spatial curvature which is created by a gravitating body with unit mass, and β describes the non-linearity of the gravitational field. These parameters influence the outcome of light deflection, gravitatonal red shift, gravitational time delay, and the perihelion shift of Mercury. Within 0.1 % these parameters agree with the values given by GR.

The parameter α is tested by red-shift experiments as $|\alpha - 1| \le 2 \cdot 10^{-4}$ using an H-maser [128]. β is determined by the perihelion advance of the Mercury as $|\beta - 1| \le 3 \cdot 10^{-3}$ [114], where the quadrupole moment of the sun is the major error source. From LLR and VLBI, β is given by $|\beta - 1| \le 3 \cdot 10^{-4}$ [37]. Finally, γ can be tested by using time delay and light deflection and can be estimated as $|\gamma - 1| \le 3 \cdot 10^{-4}$ from VLBI data [37].

Gravitational waves The direct detection of gravitational waves is one of the most important projects in physics. Beside of aiming for the first direct proof of the existence of graviational waves, gravitational wave astronomy opens a new window to the universe which enables us to study, e.g., the dynamics of black holes, the merging of black holes and the very early universe, see left part of Fig. 7 on p. 129. While Earth bound gravitational wave detectors are limited to frequencies in the 0.1 to 1 kHz range (bar detectors are sensitive to ca. 1 kHz, and laser detectors to ca. 100 Hz gravitational waves), space-born interferometers, as LISA (p. 129), and other missions like ASTROD (p. 138) are able to go down to the μHz to mHz range thus covering binary systems long before they merge. This leads to a much larger number of possibly detectable events. There are no sensitive detectors for the range from 0.1 Hz to 10 Hz.

Gravitomagnetic effects (Lense-Thrirring effect) The Lense-Thirring effect describes the dragging of an inertial frame due to the rotation of a nearby massive body predicted for the first time by Thirring and Lense [123]. There is no Newtonian analogy what thus constitutes a genuine post-Newtonian effect. This dragging effects yields a precession of a gyroscope with respect to distant stars. The total precession of the gyroscope's angular momentum is described by

$$\frac{\mathrm{d}}{\mathrm{d}\tau}\boldsymbol{S} = \boldsymbol{\Omega} \times \boldsymbol{S}\,, \tag{20}$$

with

$$\boldsymbol{\Omega} = \boldsymbol{v} \times \left(-\tfrac{1}{2}\,\boldsymbol{a} + \tfrac{3}{2}\nabla U\right) + \nabla \times \boldsymbol{h}\,. \tag{22}$$

The first term (Thomas precession) decribes the precession of the spin due to inertial forces. The second term is the gravity-induced geodetic precession due to the gravitational acceleration, the last term describes the non-Newtonian Lense-Thirring (or frame-dragging) effect, which can be interpreted as a spin-spin coupling between the gyroscope and the gravitating body rotating nearby. Another effect of the gravitomagnetic field is the motion of the knots of the ecliptic and the orbital plane of a satellite if the eccentricity of the orbit is greater than zero [25, 123].

This effect has been verified by means of an analysis of the LAGEOS satellite (p. 123 and [23, 24]) with up to 10 % accuracy. A much more precise verification within 0.1% accuracy is aimed at with GP B (p. 124 and [38]); also with atomic interferometry this effects should be measurable with very high precision (HYPER, p. 137). This effect can also be explored by means of the coupling of the frame dragging field to an elementary particle spin, see e.g. [72]. This can result in a precession of a net spin or in a Zeeman like effect for bound electrons or protons. However, these influences are too small as to be detectable in spectroscopic experiments [66].

Gravitational time delay The time delay is sensitive to the parameter γ and depends on the gravitational field strength the light passes through. In the simplest case with a Schwarzschild metric, the time delay is given by

$$\Delta\tau = \frac{4R_{\mathrm{s}}}{c}\left(1 + \frac{1+\gamma}{2}\ln\frac{4r_{\mathrm{Earth}}r_{\mathrm{refl}}}{r_0}\right), \tag{22}$$

where R_{s}, r_{Earth}, r_{refl}, and r_0 are, respectively, the Schwarzschild radius, the distance between the Earth and the Sun, the distance between the reflector and the sun, and the distance at which the light rays passes the sun. Consequently, solar system tests are most appropriate when signals sent from the Earth are reflected by another planet or a satellite. If the sun passes between Earth and reflector, the travel time of the signal increases. The observations are in agreement with GR to 0.2% [98, 113].

3.4 Condensed matter

Systems consisting of many particles are described by statistical methods which serve as theoretical tool to derive averaged quantities accessible to experiments. Such quantities are temperature, pressure, specific heat, density, etc. The basic quantity underlying the calculation of these quantities is the partition function from which everything can be derived. A method to determine and analyze the structure of the results is the renormalization group theory [41] which has also applications in other branches of physics. A main result of this theory is that critical phenomena (phase transitions) appearing by manipulating parameters show a universality and a certain scaling behaviour. That means, that near the critical tem-

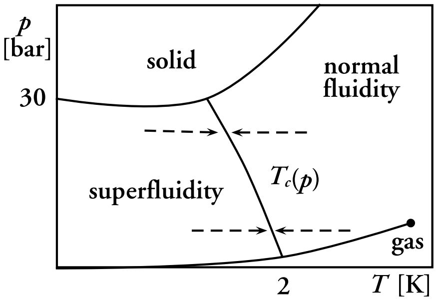

Fig. 3 Phase diagram of ^{4}He. The critical temperature T_c between the normal and the superfluid state depends on the pressure $T_c = T_c(p)$. However, when we approach the critical temperature, then thermodynamic quantities like the specific heat behave universally, independent of the pressure.

perature T_c, certain quantities describing the many particle system, like magnetization, specific heat, density, etc., behave like $\sim A^{\pm}(T - T_c)^{\beta}$. Here $A^{\pm}$ is an amplitude where the $\pm$ denotes whether the critical point is approached from above $T > T_c$ or from below $T < T_c$, see Fig. 3.

The surprising result is that the exponent β does not depend on the used particles nor on the interaction between these particles. These exponents are *universal parameters*. Furthermore, also the ratio A^+/A^- is predicted to be universal.

Another issue is that the behaviour of many particle systems should also depend on the size of the system. If L is the size if the system and t its reduced temperature $(T - T_c)/T_c$, then a characteristic quantity of the many particle system should scale according to $\lambda(L, t) \sim L^{\gamma} f_{\lambda}(tL^{1/\nu})$ where now, again surprisingly, f_{λ} depends on *one* argument only.

Best suited for an experimental study of these predictions of statistical physics and renormalization group theory is superfluid ^{4}He. Many experiments are carried out on Earth. However, gravity induces inhomogeneities in the system which limitates the accuracy of the results.

3.5 Electromagnetic interaction

The distinguished form of Maxwell's equations is very important for the validity of Special and General Relativity. Since the behaviour of light should be a consequence of Maxwell's equations, all the experiments designed to test the validity of Special Relativity, that is the Michelson-Morley and Kennedy-Thorndike, too, as well as the Doppler-shift experiments, are also tests of the Maxwell equations. Red shift and WEP experiments, too, are sensitive to modifications of these equations. In fact, as has been analyzed by Ni [85], only one particular modification of Maxwell's equations is compatible with the WEP. In other words, any modification of Maxwell's equations leads to an electromagnetically induced fifth force [40]. For a short review on the experimental foundations of Maxwell's equations, see [68]. Up to now, there does not seem to exist any complete analysis of to what extend the various already performed experiments will constrain the structure of Maxwell's equations. One ansatz for such a discussion might be the generalized Maxwell equations

$$4\pi j^{\mu} = \chi^{\mu\nu\rho\sigma}\,\partial_{\nu} F_{\rho\sigma} + \chi^{\mu\rho\sigma} F_{\rho\sigma}\,, \tag{23}$$

which have not the form as given within General Relativity, namely $\chi^{abcd} = g^{a[c}g^{d]b}$ and $\chi^{\mu\rho\sigma} = 0$, where $g^{\mu\nu}$ is the space-time metric. Compatible with the WEP is the slightly more general form $\chi^{\mu\nu\rho\sigma} = g^{\mu[\rho}g^{\sigma]\nu} + \phi\epsilon^{\mu\nu\rho\sigma}$ where $\epsilon^{\mu\nu\rho\sigma}$ is the totally antisymmetric Levi-Civita tensor and ϕ a pseudoscalar field, the so-called axion [53, 84, 85]. – The first, the 'kinetic' part in Eq. (23) is responsible for birefringence and anisotropic light propagation, while the second term may be regarded as a 'mass-tensor' because it leads to Yukawa-like modifications of the Coulomb potential.

Owing to the variety of possible effects in this generalized theory, the points discussed below will certainly not cover all the aspects needed for carrying out a complete test of Maxwell's equations, that is, tests which uniquely single out the special or general relativistic form.

Linearity of Maxwell's equations To be accurate, Maxwell's equations must be modified in order to include non-linear parts as it is predicted by the Heisenberg-Euler theory [54, 111] which is the effective theory coming out from second quantized electrodynamics in next to lowest order. Such non-linearities have been observed through light-by-light scattering [15]. There are other non-linear versions of Maxwell's equations, the Born-Infeld theory [8], for example, which was invented in order to avoid the infinities of a point-like charge. However, for ordinary laboratory experiments or experiments on a satellite such non-linearities play no role. For ordinary energies, the superposition principle of the electromagnetic field can be taken as granted to very high accuracy.

Mass of photon Even a small mass of the photon may considerably contribute to the total mass in the universe. A mass of the photon may be described my means of the Proca equation [45] where the $U(1)$ gauge invariance is broken, or in the frame of a vector valued mass which still respects gauge invariance [71]. In any case, a mass of the photon will lead to dispersion so that different frequencies propagate with different velocities. All astrophysical data and laboratory experiments limit the mass of the photon to values smaller than 10^{-50} g [107].

Birefringence of vacuum Birefringence is clearly an effect which comes from an anomalous constitutive tensor. Furthermore, also an anisotropic photon mass may lead to an energy dependent birefringence. Birefringence can be seen by observing the propagation of different polarization states of waves originating at the same event. Nothing is better here than astrophysical observations of polarized light, see [17, 53].

Charge conservation Charge conservation has many aspects: (i) The electron disappearing factor. This factor states that at most one electron will disappear within $5.3 \cdot 10^{21}$ years [119]. (ii) In [89] it is claimed that there is a strong connection between charge conservation and the Pauli exclusion principle in the sense that one of these principles cannot be violated without a violation of the other. (iii) The neutrality of atoms or the equality of electron and proton charge which has been confirmed to $|1 - e_e/e_p| = 0.8 \cdot 10^{-19}$ [120], and the neutrality of the neutron which is tested to $q_n \leq 5 \cdot 10^{-18}e$ [117]. The first result only states that the electron and proton charges are equal but still may change their abosulte values. (iv) A time-dependence of the fine structure constant $\alpha = e^2/\hbar c$. A measurement of a hypothetical time dependence of the fine structure constant can be obtained by comparing different time or length standards which depend in a different way on

α. In the laboratory experiments treated in [95], variations of the fine structure constant can be detected by comparing rates between clocks based on hyperfine transitions in alkali atoms with different atomic numbers. The comparison of the H-maser with a Hg^+-clock resulted in $d\alpha/\alpha \leq 3.7 \cdot 10^{-14}$. In a new proposal the time-dependence may be measured with very high precision using monolithic resonators [109]. (v) In the frame of the generalized Maxwell equations, a charge non-conservation is connected with a photon mass tensor [71]. (vi) The behaviour of atomic clocks: Since any modification of the potential of a point charge modifies the structure of the atomic energy levels, spectroscopy or the time given by an atomic clock also reflects a charge non-conservation. Furthermore, since the atomic clocks are sensitive to the fine structure constant, a charge non-conservation in addition gives rise to a temporal change in the energy levels.

Quantum gravity modifications In general, quantum gravity leads to space-time fluctuations which will modify the dynamics of fields in space-time. Since quantum gravity induced modifications of Maxwell's equations in most cases can be described within the frame given by Eq. (24), thus leading to birefringence and dispersion. The quantum gravity modified dispersion relation in general has the structure

$$\boldsymbol{k}^2 = \omega^2 \left[1 + \xi \left(\frac{\omega}{\omega_{\rm QG}} \right)^{\alpha} + \mathcal{O} \left(\frac{\omega}{\omega_{\rm QG}} \right)^{\alpha+1} \right], \tag{24}$$

where ξ is a parameter which depends on the underlying quantum gravity theory ($\xi^{(\rm string)} = 3/2$, $\xi^{(\rm loop)} = 4$) and $\omega_{\rm QG}$ is a quantum gravity energy scale which is assumed to be of the order of the Planck energy. The corresponding velocity of light

$$c_{\rm QG} = c \left(1 - \xi_{(1)} \frac{\omega}{\omega_{\rm QG}} \right) \tag{25}$$

depends on frequency. This can be tested best with high energy photons coming from gamma ray bursts [3, 4], for example.

Furthermore, due to this dispersion relation, high energy photons interact with the cosmic microwave background photons leading to a creation of particles. Therefore the original photon looses energy. Thus the free path of such high energy photons is limited to the order 100 Mpc. However, this so-called GZK-cutoff (Greisen-Zatsepin-Kuzmin) [47, 136] does not seem to exist thus supporting the hypothesis of a quantum gravity modified dispersion relation, see e.g. [96].

3.6 Weak interaction

Parity violation in molecules There are theoretical predictions that due to the existence of the weak interaction right- and left-handed versions of molecules give rise to slightly different energy levels, see [43] for a recent review. There are experimental proposals to test these slight difference spectroscopically [29].

Though the violation of parity has been observed in many physical systems, a violation of the invariance of physics against time reversal has been detected only once up to now. A violation of time reversal is connected with the existence of a permanent dipole moment of elementary particles. Since it is not yet understood which physical mechanism may be responsible for time reversal, a search for an electric dipole moment [97] may shed more light on this problem. Experiments of this kind have the capability to change the standard model.

3.7 Strong interaction

The exploration of the physics of the strong interaction needs high energies and thus huge accelerators. Even higher energies of up to 10^{21} eV are available in space. (Though it is a very interesting and strongly evolving area of modern physics, the detection of high energy cosmic rays in space are just observations and no experiment with a well defined experimental setting of initial conditions. Therefore we are here not concerned with it.)

Recently, experiments on the anomalous g-factor of the muon [11, 90] have revealed a discrepancy of theoretical predictions of the standard model and experimental results. Though the data needs to be confirmed, there are speculations that a relation to supersymmetry is the most plausible explanation for this result [39].

4 Why Fundamental Physics in Space

Space conditions

- infinitely long free fall
- large velocity differences
- large grav. potential differences
- long distances
- low noise

In most cases it is possible to perform very high precision experiments on Earth. This is so, because in many experiments the gravitational field plays no role and the seismic noise is either irrelevant or can be shielded well enough. However, the more precise the experimental devices will be, the more the environment on Earth becomes the most disturbing part in experiments. In addition, some experiments really need an interaction-free environment which also includes absence of any acceleration and rotation. Consequently, we have two categories of reasons for trying to do experiments not on Earth but instead in space: Basic reasons and technical reasons.

4.1 Basic reasons

The fundamental reasons for performing experiments in space are that there are conditions which in principle cannot be achieved on Earth. Such conditions are the *space conditions* which consist of

- an environment where gravity is nearly compensated and we have a free fall for a very long time and long interaction times (under weightlessness),
- large changes in the velocity,
- large potential differences, and
- long distances.

On Earth, the free fall may have a duration of up to several seconds in a drop tower, and up to 20 seconds in a parabola flight. However, in an airplane there are big residual accelerations hinting to do high precision tests. A long free fall of bodies and particles is very important for tests of the WEP (MICROSCOPE, STEP, GG). A long interaction time is also important for interference experiments, e.g. HYPER. This is not possible on Earth because the interfering particles will fall out of the interferometer after a short time. Even the small rotation of the Earth's surface may influence some experiments like spectroscopic experiments aimed to search for anomalous spin–couplings. Therefore, for many experiments a non–rotating, non–accelerating frame is very important. It can be achieved in space only.

Furthermore, changes in the velocity of macroscopic bodies on Earth can be merely of the order of 1 km/s (elementary particles, of course, can be easily accelerated to velocities very close to the velocity of light). For larger changes one has to go to space. There one may achieve a change of the velocity of the order of 10 km/s, but even higher. This is of advantage for tests of Special Relativity: large changes of the velocity improve the accuracy of the experimental result (SUMO, OPTIS).

Absolutely clear is that large differences in the gravitational potential can be achieved only in space. The difference in height on the Earth is of the order of 20 km which can be obtained by aircrafts or balloons. Much larger values can be obtained in space by means of highly eccentric orbits. And even larger potential differences can be obtained by high eccentric solar orbits. Such orbits are indeed under consideration for missions testing the universality of the gravitational red shift (SpaceTime), because the effect searched for scales with the potential difference the clocks experience during flight.

As a last and again obvious point we add that extremely large distances which are of use in detectors for low frequency gravitational waves or VLBI in space, for example, can be established in space only (LISA, ASTROD).

4.2 *Practical reasons*

Many FP experiments must be carried out in the low frequency range ($< 10^{-3}$ Hz); like the satellite projects LISA, MICROSCOPE, STEP, for example. On Earth, seismic noise dominates the low frequency range. Although damping systems, like multiple pendulum suspensions, and active seismic control by means of closed feedback-loops can help to reduce the mechanical disturbing vibrations very effectively, the cut-off frequencies for a typical Earth-bound laser interferometer is between 10 and 100 Hz. Nevertheless, measurements on satellites do not guarantee necessarily a reduction of the noise bandwidth. Periodic disturbing effects like systematic variations during one orbit, strong temperature variations, or radiation become influential in the low frequency range, but can be eliminated by a proper choice of orbit and spin rate, as well as precise attitude control to attain levels of residual accelerations down to 10^{-14} m/s^2.

Nearly perfect vacuum conditions in high orbits make it often easy to carry out an experiment in space, in particular if spacecrafts are in formation flight and are linked by laser beams over very long distances.

Space enables us to build up experiments with extremely large extensions. The armlength of LISA will be about 5 million km, which will result in an enormous sensitivity. Also measurements over long distances between the Earth and deep space satellites are possible and enable to map out gravitational fields and space-time curvature by time delay measurements. The *Viking* Landers on Mars in 1974 have been used for these post-Newtonian gravity tests; *Pioneer10* launched in 1976 is still active (with a present signal travel time of about 16 min). Also several new planned missions, like ASTROD for determining post-Newton parameters with a precision 3 to 6 orders of magnitude higher than available today, are based on long distance measurements. For these missions the signals on the way between Earth and satellite sometimes have to pass the solar gravitational field thus making delay time measurements possible.

5 New high-precision experimental techniques

Atomic interferometry With atom interferometers it is possible to determine very precisely phase shifts due to acceleration or rotation [5–7]. This results in the development of atom interferometer based accelerometers and gyroscopes. The present day sensitivity of atom interferometers used as accelerometer is $\delta a \sim 10^{-9}\ \mathrm{m}/(\mathrm{s}^2\sqrt{\mathrm{Hz}})$ [93] and as gyroscope $\delta\omega \sim 6 \cdot 10^{-10}\,\mathrm{rad}/(\mathrm{s}\sqrt{\mathrm{Hz}})$ [49]. With atom interferometers, also a very precise measurement of $\hbar/m$ is planned. Furthermore, it has the capability to measure the Lense-Thirring effect and to explore the WEP in the quantum domain (see the HYPER project, p. 137).

H-maser A clock with an accuracy of 10^{-15}. This kind of clock has been used for the most precise verification of the gravitational red shift (GP-A).

Cavities and resonators Optical resonators are today the most stable length standards. For cryogenic resonators, the stability is given by $\Delta l/l \leq 2.3 \cdot 10^{-15}$ over 20 s [112]. The cavities can be made of ULE (Ultra Low Expansion) materials with thermal expansion coefficients of $10^{-9}/\mathrm{K}$ or of Silicon which possesses a vanishing thermal expansion coefficient at 140° K. Frequency drifts due to aging effects can be reduced to the order of 1 Hz per day.

Ultrastable lasers Laser light with very high intensity stability and frequency stability can be produced by diode-pumped Nd:YAG lasers. Such lasers have already been proven to be space-qualified and are planned to be used in LISA.

Atomic clocks Space-qualified atomic clocks based of Rubidium or Cesium are already used in space. Their intrinsic stability is of the order 10^{-15}.

Optical frequency comb This recently invented device is of great importance for further improvements of Kennedy-Thorndike tests as well as for tests of the Universality of the Gravitational Red Shift. With the help of a mode-locked femtosecond laser emitting a series of very short laser pulses with a well-defined repetition rate, a frequency comb can be generated which makes it possible to compare the microwave frequency of atomic clocks (about 10^{10} Hz) with optical frequencies (about 10^{15} Hz) with an accuracy of 10^{-15} [30].

SQUIDs (Superconducting Quantum Interference Devices) SQUID based measurement rely on two phenomena: (i) the flux quantization in superconducting loops and (ii) the Josephson effects. Both effects are only observable in presence of superconductivity. A SQUID is the most sensitive magnetic flux detector known today. Because almost any low-frequency signal, that can be converted into a corresponding magnetic flux, can be detected with very high precision. Therefore, a lot of applications of SQUIDs in modern experimental physics are known. For fundamental physics, SQUIDs are mainly used to measure positions as well as linear and angular accelerations. For these measurements, any test mass movement induces an inductance signal coupled to the SQUID [129].

Drag-free concept Drag-Free Attitude and Orbit Control (AOCS) is a powerful tool to fly a satellite on a nearly perfect geodesic. Normally, the movement of any satellite along its orbit is disturbed by many effects. The biggest effect in a low Earth orbit is the drag of the rest-atmosphere. But also other effects, like the Earth's magnetic field, the solar radiation pressure, cause forces and torques which prevent the satellite to be in perfect free fall. Drag-free AOCS is based on a reference sensor consisting of a freely falling mass hindered to touch the cage by a closed loop control and appropriate thrusters controlable down to 0.1 μN.

FEEPs (Field Emission Electrical Propulsion) FEEP is a thrust concept to attain very low thrust levels for drag-free AOCS. The propulsion system is based on the acceleration of Cesium or Indium ions in a high voltage positive electric field. The systems are very small and ideal for long term missions. More information can be found on the homepage of the Austrian Research Centers Seibersdorf `http://www.arcs.ac.at/E/EM/ultra`.

6 FP missions related space agencies

In the next two sections we are presenting the past missions, the missions under development, and the missions under study. A mission under construction is finally

space agency		country	general web page
ESA	European Space Agency	Europe	`http://sci.esa.int` `http://sci.esa.int/home/ourmissions/index.cfm`
NASA	National Aeronautics and Space Administration	USA	`http://www.nasa.gov` `http://spacescience.nasa.gov/missions/index.htm`
DLR	Deutsches Zentrum für Luft- und Raumfahrt	Germany	`http://www.dlr.de`
CNES	Centre National d'Études Spatiales	France	`http://www.cnes.fr`
ASI	Agenzia Spatiale Italiana	Italy	`http://www.asi.it`
NASDA	National Space Development Agency	Japan	`http://www.nasda.go.jp/indexxe.html`
IKI	Russian Space Research Institute	Russia	`http://www.iki.rssi.ru`
BNSC	British National Space Centre	UK	`http://www.highview.co.uk/`

approved and will fly definitely. A mission under study may have a certain status within ESA or NASA or any other space agency, and may get support in order to develop technology necessary for the mission, but there is no final decision up to now that this mission will fly.

General information about space projects can be found on the web pages of the various space agencies (see table on page 120).

7 Past FP missions

Mission		Launch date	Space agency
GP-A	Gravity Probe A	1976	NASA
Viking		1976–82	NASA
LLR	Lunar Laser Ranging	1969–present	NASA
LAGEOS I & II	Laser Geodynamics Satellite	1992–present	NASA

7.1 GP A (Gravity Probe A)

Scientific Objectives: GP-A was the first FP mission in space. Its purpose was (i) to measure the Gravitational Red Shift by means of a H-maser clock, and (ii) to demonstrate the first use of H-masers for a space experiment, that is, the function of a maser clock in space.

Experimental Payload: The payload consisted of a H-maser in the space probe and on ground on an S-band transmitter phase-locked to the maser, and an S-band transponder.

Mission Scenario: The space probe GP-A has been launched on a ballistic trajectory. After launch, GP-A was in space for one hour and 55 minutes in an elliptical flight trajectory with a maximum height of ca. 10,000 km above the Earth. Essential in this experiment was the implementation of a Doppler-cancellation scheme by means of the ground H-maser and the S-band transmitter and transponder in the space probe. This cancellation scheme lead to the elimination of first order Doppler effects. By tracking the space probe within a range of 100 m and incorporating various frequency changes due to the atmosphere a precise determination of the frequency shift within $5 \cdot 10^{-15}$ makes it possible to determine the gravitational influence on the frequency.

Technology: H-maser on Earth and in the space probe, and microwave links between space probe and H-maser on Earth.

Result: The gravitationally induced red shift given by Eq. (15) has been confirmed to 0.1% accuracy: $|\alpha_{\text{H-maser}}| \leq 10^{-4}$.

Further information: [127, 128],
`http://einstein.stanford.edu/genxint/faqs/gpaxvessot.html`.

7.2 Viking

Scientific Objectives: Beside other objectives concerning the exploration of Mars, on Viking (1976) also an experiment has been carried out to improve earlier measurements of the gravitational time delay on Mariner Missions in the early seventies.

Experimental Payload: Communications were accomplished through a 20 W S-band transmitter and two 20 W TWTA's. A 2-axis steerable high-gain parabolic antenna was mounted on a boom near one edge of the lander base. An omnidirectional low-gain S-band antenna also extends from the base. Both these antennae allowed for communication directly with the Earth.

Mission Scenario: Signal time delays has been measured between the Viking landers and the Earth. Although the effects of the intervening solar wind complicated the experiment, it could be clearly demonstrated that the radio signals took longer on their round trip by just the amount given by the predicted slowing of time. Due to the communication system, the influence of the sun's atmosphere on the travel time of light could be eliminated.

Further information: [98].

7.3 LLR (Lunar Laser Ranging)

Scientific Objectives: (i) Search for the Nordtvedt effect which is an indication of a violation of General Relativity. (ii) Testing for a Yukawa-like gravitational field at Earth-Moon distances. (iii) Search for a time-dependence of the gravitational constant, (iv) for preferred frame effects (violation of Special Relativity), (v) test of the space-curvature described by γ, and (vi) of the non-linearity parameter β.

Experimental Payload: This experiment used several LRRRs (Laser Ranging RetroReflector) which consisted of an array of fused silica cubes, arranged to reflect a beam of light back on a parallel path to its origin. The LRRR placed on the Moon, see Fig. 4, was aligned precisely so that it faced the Earth. Laser beams from the Earth are reflected back to Earth. The Apollo 11 apparatus is in operation since 1969.

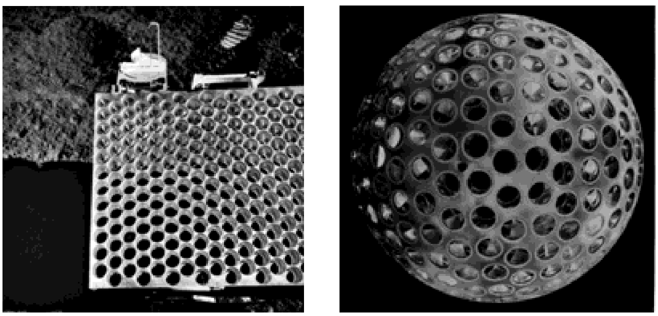

Fig. 4 **Left:** The Laser Retroreflector of the Apollo 15 mission. It is a 46 cm square aluminium panel with 100 fused silica half–cubes, each hyaving a diameter of 3.8 cm **Right:** The LAGEOS satellite with its 426 cube–corner retroreflectors. The satellite is only 60 cm in diameter. 422 of the retroreflectors are made by fused silica, 4 are made of germanium and may be used by future lasers.

Mission Scenario: Five laser retroreflectors have been placed on the moon by the U.S. Apollo 11, 14, 15, missions and by the Russian Luna 17 and 21 missions which placed French reflectors on the moon. However, the Luna 17 reflector was covered by dust and could not be used for observations. Since from 10^{19} photons which are sent from Earth to the Moon less than one comes back, a special data analysis had to be developed.

Technology: It needed enormous efforts to improve the laser measurement resolution by a factor of 1,000 over the last 3 decades. Today's measurements are carried out on McDonald Observatory (Univ. of Texas, Fort Davis), on Mount Haleakala on the Hawaiian island Maui, and on the Observatoire de la Côte Azur in Grasse, France. Single photons can only be detected by comparison of their arrival time with a pre-calculated one. Only photons with less than 30 ns arrival time deviation are considered for further evaluations. Ca. 100 of these events related to about 15 min of observation time are used to define one measurement point.

Results: The resolution for Earth-Moon distance mesaurements attainable today is in the range of 3 cm. The evaluation models take into account all known relativistic effects as well as the relative movements of the Sun, the Earth, the Moon, all planets, and the major asteroids [132]. These models are based on an isotropic PPN-*n*-body metric. The Nordtvedt parameter can be determined to an accuracy of -0.0007 ± 0.0010 [132] related to a proof of the Strong Equivalence Principle of 1 part in 1,000. In addition, various PPN parameters can be determined with high accuracy, $\gamma = 0.99994 \pm 0.00034$, $\beta = 0.99981 \pm 0.00026$, $\alpha_1 = 0.00008 \pm 0.000009$, and $\alpha_2 = 0 \pm 0.000025$, see [37, 118].

Further information: [88].

7.4 LAGEOS (LAser GEOdynamics Satellite)

Scientific Objectives: Satellites have been launched to serve as reference for position measurements on Earth which are used for determining the motions (i) of tectonic plates, (ii) of shifts of the Earth's rate of rotation and (iii) of the Earth's gravitational field. These satellites has recently been used for the determination of the Lense-Thirring effect on the orbits of the satellites.

Experimental Payload: The satellites consist of a metallic sphere with 426 glass reflectors, see Fig. 4 (right side).

Mission Scenario: LAGEOS I was launched in 1976 and LAGEOS II in 1989. Both were brought into nearly circular orbits (eccentricity = 0.0045). The orbit height is 5,900 km and the inclination for LAGEOS I is 110° and for LAGEOS II 152°, respectively. The progression of the perigee of 3.3 arcsec per year, which is due to the Lense-Thirring effect, can be calculated. A third satellite is planned to be launched.

Technology: No special technology is used since this is a passive satellite. The vehicle has no onboard sensors or electronics, and is not attitude controlled.

Further information: [22–24], `http://galileo.crl.go.jp/ilrs/lageos.html`.

8 FP missions under development

Mission		Projected launch date	Space agency
GP-B	Gravity Probe B	2002	NASA
MICROSCOPE	Test of the WEP	2005	CNES-ESA
SUE	Superfluid Universality Experiment		NASA-DLR
BEST	Boundary Effects near Superfluid Transitions		NASA-DLR

8.1 GP-B (Gravity Probe B)

Scientific Objective: Gravity Probe B (GP-B) is a NASA project to test two so-called gravitomagnetic effects of General Relativity predicted by Lense and Thirring [123]. The goal of GP-B is to observe non-Newtonian precessions of gyroscopes in Earth orbit given in Eq. (20). This Lense-Thirring (or frame-dragging) effect is shown in Fig. 5. On a satellite in a circular polar orbit of about 640 km, the geodetic precession of the gyroscope is ca. 6.6 arcsec per year, and the perpendicular Lense-Thirring precession is in the order of 0.041 arcsec per year. For a complete theoretical description see e.g. [72]. Both effects can be measured on GP-B with an accuracy of 2 parts in 10^5 for the geodetic precession, and of 0.3% for the Lense-Thirring effect.

Experimental Payload: The experiment consists of 4 gyroscopes with their spin axes aligned parallel to the line of sight to a far distant guide star representing the cosmic reference frame. The gyroscopes are mounted in a quartz block and rigidly

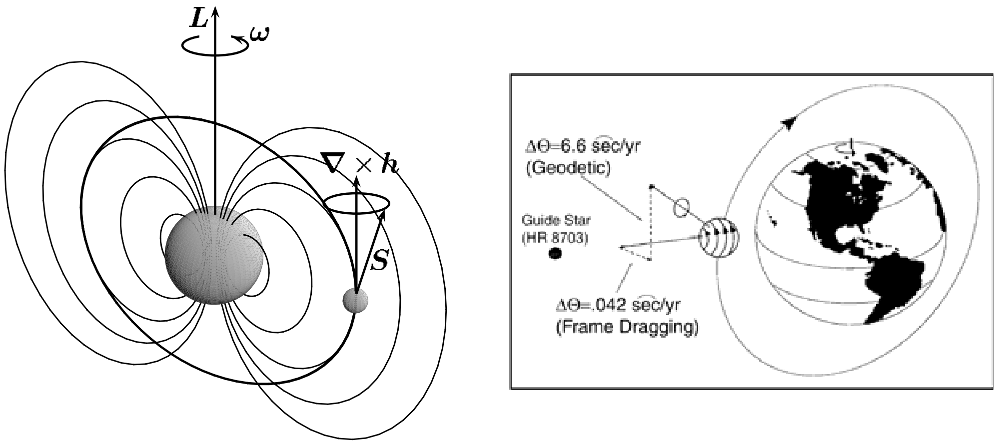

Fig. 5 The Lense–Thirring effect for gyroscopes: The Earth rotating with angular velocity $\boldsymbol{\omega}$ and angular momentum $\boldsymbol{L}$ creates a gravitomagnetic field with the shape of a magnetic dipole. A gyroscope with angular momentum or spin $\boldsymbol{S}$ moves around the Earth along a geodesic circular polar orbit (thick solid line). The Lense-Thirring effect consists in the precession of $\boldsymbol{S}$ around the direction given by the field lines of $\nabla \times \boldsymbol{h}$ and can be measured by comparison of the spin's direction with a reference star.

attached to a Casssegrain telescope tracking the guide star. The gyroscopes are fused quartz spheres of about 40 mm diameter coated with a superconducting niobium film. The rotating spheres (spin rate is about 100 Hz) are suspended by electrostatic forces and are, therefore, surrounded by adequately shaped electrodes. The measurement of the precession rate is based on a superconducting effect, called the London moment. A spinning superconductor develops a magnetic field directed along the initial spin axis. This field direction serves as base line, and any precession induces a moment which can be measured magnetically by a SQUID-based magnetometer. To make the system sensitive enough to measure the weak inductance signals, a special magnetic shielding with pre-cooled and expanding superconducting lead bags levels the magnetic fields to less than 10^{-11} T. To attain superconducting conditions, the quartz block has to be cooled down and is enclosed in a Dewar vessel containing 2,400 l of liquid helium. Spinning the spacecraft around the line of sight to the guide star modulates the science signal and reduces limits from $1/f$ noise. For roll rates of some mHz, the noise is betwen 10^{-28} to 10^{-29} J/Hz which results in a static resolution of about 0.001 arcsec for an integration time of 7 hours. Considering additional errors from gyroscope drifts, SQUID-readout, and uncertain guide star movements, an overall accuracy for one gyroscope of 0.00026 arcsec per year, and of 0.000018 arcsec per year for measurements with all four gyroscopes can be attained. It is worth to notice that this resolution is 7 orders of magnitude better than usual inertial navigation gyroscopes perform. A comprehensive description of the experimental hardware can be found in [38].

Mission Scenario: The GP B satellite will be launched in a circular polar orbit with an orbital height of 640 km; the launch is scheduled for fall 2002. The main structural element of the spacecraft is the huge Dewar vessel. All spacecraft subsystems are mounted on a welded aluminum frame fitting around the lower end of the Dewar. The total weight of the satellite is about 3,300 kg. Because the drift rate of the gyroscopes is depending on torques, like mass-unbalance, gravitational attraction of the satellite etc., the drag by rest atmosphere disturbing the satellites movement on an ideal geodetic has to be compensated. A special drag-free attitude and orbit cotrol system has been developed reducing the residual acceleration level acting on the gyroscope to less than 10^{-13} m/s^2 in the mHz range. Therefore a mass-trim mechanism and specially developed 16 helium proportional thrusters are used for attitude and orbit control able to attain thrust control down to the sub-mN range. To attain this high precision of thrust control, the helium boil-off from the Dewar vessel is directed continously through pairs of opposed nozzles. By applying this method, the gas flow through the nozzles can be controlled with a single valve whose shift increases the flow through one nozzle and decreases the flow through the other nozzle simultaneously. The outgasing rate of some mg per s guarantees a low Reynolds number regime and, therefore, a very smooth control. The pointing accuracy (meeting the line of sight to the guide star) is better than ± 20 marcsec. The residual acceleration acting on the satellite meets the requirement; and the roll rate can be controlled with a relative accuracy of 1 part in 10^5. Translation control and mass-trim system guarantee that the centre of spacecraft rotation and the line through the gyroscopes do not deviate more than 50 μm.

Technology: A number new experimental and space technologies had to be developed for GP-B. GP-B will be the first satellite with low-T_c SQUID-based sensing technology enabling to use the most precise gyroscopes ever built. The operation of SQUIDs is based on two effects: (1) the flux quantization in superconducting loops and (2) the Josephson effect. A SQUID is the most sensitive magnetic flux detector known today. Its basic principle is that the tunneling of Cooper pairs through a small gap in a superconducting ring is depending on the magnetic flux perpendicular to the ring. However, the application of SQUIDs is not restricted to magnetic flux measurements only. Almost any low-frequency signal can be detected by SQUIDs with very high sensitivity.

GP-B will also be the first scientific satellite with drag free control which will become a standard space technology of many other satellites for fundamental physics experiments. It is remarkable that for GP-B the classical concept of strict separation of satellite system and experiment is not longer existing. The drag-free control makes it necessary that the experiment is completely within the thuster control loop. The unique combination of challenging experimental and space technologies makes GP-B not only an outstanding gravitational experiment, but also a precursor of other fundamental physics missions.

Further information: [38], `http://einstein.stanford.edu/`.

8.2 MICROSCOPE (Micro-satellite à traînée Compensée pour l'Observation du Principe d'Équivalence)

Scientific Objectives: Free fall experiments on the French satellite MICROSCOPE will test the WEP to an accuracy of $\eta < 10^{-15}$. η is defined in Eq. (6). Best tests caried out in laboratory with torsion pendulums could test the WEP with an accuracy of only 10^{-12}. Lunar laser ranging experiments attained a similar level of accuracy. Also terrestrial drop tower experiments can attain 10^{-13} best. Free fall experiments in space take advantage of an extremely low level of residual accelerations acting on test masses and enable long term signal integration. In usual Galileo-type free fall experiments the relative motion of two free falling test masses made from different materials has to be compared. The WEP test on MICROSCOPE is performed by controlling the relative motion of both test masses at null so that any WEP-violation appears through the measured forces necessary to nullify this relative motion. The experimental baseline of MICROSCOPE is to carry out the experiments on-board a drag-free satellite with two servo-controlled electrostatic accelerometers, one implemented inside the other one. Thus, the two test masses are centred to avoid influences of gravity gradient fluctuations. The configuration senses differential accelerations acting on both test masses.

Experimental Payload: The payload consists of two of these differential accelerometers to be operated at room temperature. Test masses of the first differential accelerometer have cylindrical shape and are made from platin and tantal, respectively. The second differential accelerometer contains two cylindrical test masses both made from platin to enable the measurement of systematic errors. The cylinder symmetry axis is directed inside the orbital frame (x-axis), resulting in a signal variation periodic with orbit frequency in the case of WEP-violations. The satellite itself spins about the axis perpendicular to the orbital plane (y-axis) varying the orientation of the Earth's gravity field in the instrument reference frame and enabling to discriminate systmatic disturbances. With a signal integration over 20 orbits (100,000 s), differential accelerations will be measured with a resolution of 10^{-15} m/(s$^2\sqrt{\text{Hz}}$) at the sum of orbital and spinning frequency which will be about 10^{-3} Hz. A 10^{-15} rejection of the accelerations applied in common mode of the test masses leads to a 10^{-8} m/(s$^2\sqrt{\text{Hz}}$) requirement for the drag-free compensation. The satellite mass will not exceed 120 kg, payload power will be less than 40 W.

Mission Scenario: The satellite is designed to be launched as an ARIANE 5 — ASAP payload in 2004. The satellite will fly in a circular polar orbit of 600 to 700 km height. The orbit has an eccentricity of less than 10^{-3}. Orbital plane and Sun-Earth axis cover an angle of about 20°. Because the satellite's spin axis is stabilized perpendicular to the orbital plane, the satellite is not sun-pointing. MICROSCOPE is a drag free satellite. The thrust system for drag and torque compensation consists of 4 clusters of 2 field electrical emission propulsion systems (FEEPs) giving a thrust to be controlled from 0.1 to 20 μN range.

Technology: The accelerometer development is based on long term experience in ultra-high precision electrostatic (capacitive) sensors for space missions at the Office National d'Etudes et de Recherches Aérospatiales (ONERA). These sensors are constructed around a high density proof mass with a very fine and stable silica gold coated core. Position and attitude of the proof mass is measured with capacitors. The proof masses are controlled with electrostatic actuators. Instruments with different resolution of this type have been flown already on other missions. On MICROSCOPE for the first time, two accelerometers are combined to a quasi-differential accelerometer. A servo-controlled electrostatic accelerometer measures the electric force necessary to maintain a test mass motionless with respect to the cage. Test mass and capacitor form a spring-mass system, and the sensor resolution is depending on the stiffness.

Further information: [125], `http://www.onera.fr`, `http://www.cnes.fr/activites/connaissance/physique/1index.htm`.

8.3 SUE (Superfluid Universality Experiment)

Scientific Objectives: Study of phase transitions that occur when helium is supercooled into a liquid and furthere cooled into a superfluid, in a microgravity environment under different pressures. In more detail: SUE will measure the superfluid density at various pressures near the lambda line of helium and from this (i) the sound velocity along isobars, (ii) the heat capacity, and (iii) the damping coefficient.

Experimental Payload: The volume of the experimental payload is of about 1 liter and is surrounded by an outer Niobium cylinder in order to shield stray magnetic fields.

Mission Scenario: The experiment will be placed on an exterior test platform (Low Temperature Microgravity Physics Facility, LTMPF) of the ISS.

Technology: SUE needs an ultrahigh-precision, superconducting pressure sensor and regulator, a low-dissipation thermal-wave oscillator, an ultralow-noise thermal wave detector and a thermal control in the nK range.

Further information: `http://chex.stanford.edu/sue/`, `http://funphysics.jpl.nasa.gov/technical/ltcmp/sue.html`.

8.4 BEST (Boundary Effects near Superfluid Transitions)

Scientific Objectives: Study of molecular-level boundary issues using liquid helium during a phase transition between fluid and superfluid states in gravity-free environment. In detail: BEST will (i) improve the measurement of the thermal conductivity in a three-dimensional ^{4}He sample along the lambda line by three orders of magnitude, (ii) measure the thermal conductivity of ^{4}He in one- and two-dimensional confinements of various sizes, and (iii) examine the cross-over behaviour from three-dimensional superfluid transitions to the fundamentally different two-dimensional superfluid transitions.

Experimental Payload: Superfluid helium in various boundary conditions given by e.g. microchannel plates, see Fig. 6, together with thermometers and pressure regulators.

Mission Scenario: This experiment is planned to be carried through on the ISS.

Technology: In order to explore small sizes of Helium samples, one needs small high-resolution thermometers, high-precision sensors, and high-precision thermal control. In order to perform the tests on one- and two-dimensional constrained helium samples one needs confinement media with very high uniformity and low thermal conductivity.

Further information: `http://titanium.qi.ucsb.edu/~best/`, `http://funphysics.jpl.nasa.gov/technical/ltcmp/best.html`.

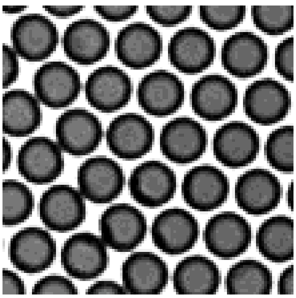

Fig. 6 A microscope image of a microchannel plate serving as finite–size confinement medium for superfluid Helium.

9 FP missions under study

Mission		Projected launch	Space agency
LISA	Large Interferometer Space Antenna	2011	ESA-NASA
ACES/PHARAO	Atomic Clock Ensemble in Space	2005	CNES/ESA
STEP	Satellite Test of the Equivalence Principle	2005	NASA-ESA
SUMO	Superconducting Microwave Oscillator	~2006	NASA
STM	Space–Time Mission		NASA
HYPER	Hyper Precision Atom Interferometry in Space	>2015	ESA
OPTIS	Optical Test of Special and General Relativity		DLR
ASTROD	Astrodynamical Space Test of Relativity using Optical Devices		
WEAX	Weak Equivalence Principle for Antimatter		ESA
SEE	Satellite Energy Exchange		NASA
GG	Galileo Galilei		ASI

9.1 LISA (Laser Interferometer in Space Antenna)

Scientific Objectives: The objective of the Laser Interferometer Space Antenna (LISA) mission is to measure gravitational waves in the frequencey range between 10^{-4} and 10^{-1} Hz. Data in this frequency range are expected from massive black holes, black hole formation, black hole binary coalescence, and galactic binaries, see Fig. 7

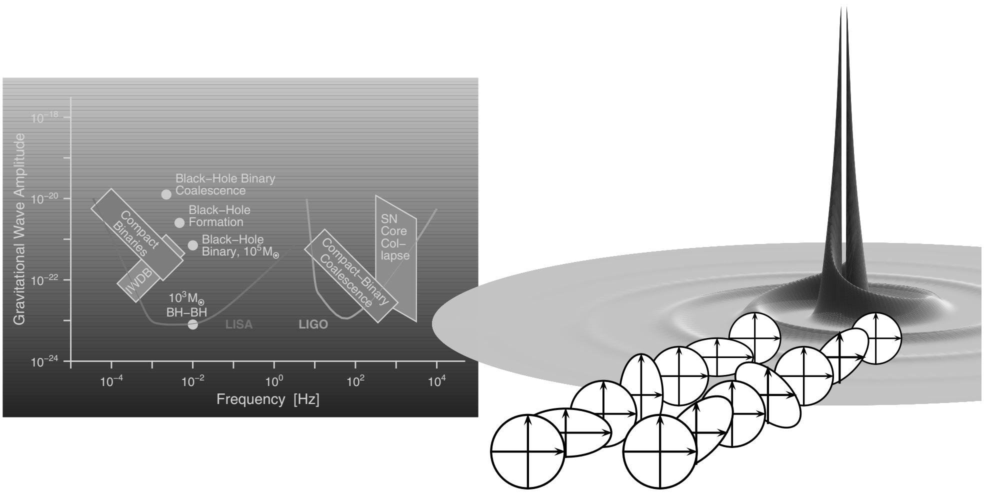

Fig. 7 The detection of gravitational waves. **Left:** Sources of gravitational waves for terrestrial and space detectors. No detectors sensitive enough are available for 0.1–10 Hz. **Right:** An inspiraling binary system creating gravitational waves of two different polarizations. The arrows vizualize the interferometer arms being contracted and elongated under the influence of the gravitational wave, and a set of freely falling particles originally positioned on a ring will be deformed to ellipses. In the case of the orientation of the interferometer arms as shown, the +-polarization (left) exerts the maximal distortion, for the ×-polarization (right) this interferometer is insensitive.

left. This frequency range cannot be covered with ground-based detectors, because of unshieldable seismic noise on Earth and a limitation in their spatial extension to some kilometers only. The mission's goal is not only to detect gravitational waves, but also to observe them systematically over a 2 (minimum) to 10 years (maximum) period. The strain sensitivity of the interferometer is $h/2 = \delta L/L = 4 \cdot 10^{-21}$ at a signal frequency of 10^{-3} Hz. This implies that after an integration time of about one year one achieves a sensitivity of $h = 10^{-25}$. Another goal is – perhaps together with other gravitational wave detectors – gravitational wave astronomy. From that one expects a lot of information about the physics of black holes and of the very early Universe. This is possible because, in contrast to electromagnetic radiation, gravitational waves cannot be shielded.

Experimental Payload: The LISA mission consists of three identical spacecrafts arranged in an equilateral triangle formation and separated by about 5 million km. Each spacecraft carries two phase-locked laser systems and two mirrors. Two sides of the triangle are the giant arms of a Michelson interferometer as it is used for ground-based detectors, too. The third arm is added for redundancy and enables to get independent information about wave polarisation. The light from a Nd:YAG laser with a wavelength of 1.064 μm and an output power of about only 1 W of any spacecraft is directed to the other two spacecrafts. The mirrors are actively driven by phase locking so that the phase information of the detected photons are used to control the phase of the outgoing light. The interferometer fringe resolution is about $4 \cdot 10^{-5}\,\lambda/\sqrt{\mathrm{Hz}}$ ($\lambda = 1064\,\mu$m is the wavelength of the used laser light), providing a frequency stabilization of $30\,\mathrm{Hz}/\sqrt{\mathrm{Hz}}$ with a Fabry-Perot reference cavity. Each mirror is a electrostatically controlled drag-free reference mass (see the description of the MICROSCOPE mission) which guarantees that the entire interferometer is on a geodetic. The spacecraft, therefore, serves as a drag shield against the light pressure of about $5 \cdot 10^{-6}\ \mathrm{N/m^2}$, the biggest source of disturbance. The mirrors, $40 \times 40 \times 40\ \mathrm{mm}^3$ cubes, are made from Au-Pt alloy with extremely low magnetic susceptibility, and are placed inside a vacuum chamber see Fig. 9.

Mission Scenario: The center of mass of the spacecraft triangle moves on a heliocentric orbit with one 1 year duration trailing the Earth by 20°. The spacecraft triangle is inclined 60° with respect to the ecliptic and the triangle as a whole rotates around its centre of mass, see Fig. 8. The rotation of the triangle and the 1 year orbit around the sun enables to identify the source direction by the observation of Doppler-shift effects. Drag free control for each spacecraft will be done with an accuracy of $3 \cdot 10^{-15}\ \mathrm{m/s^2}$ in the signal frequency band with 6 clusters of 4 FEEPs each (for further description see the MICROSCOPE project). The pointing performance attainable is less than $10\ \mathrm{nrad}/\sqrt{\mathrm{Hz}}$. The spacecrafts will be launched together and separated later for individual orbit injection. Therefore, each spacecraft carries its own ion-propulsion system. Current launch date is 2011.

Technology: New technologies flown on LISA are the high performance laser system, the extremely ambitious drag-free control of the satellites, as well as the extremely wide range interferometry. Therfore, ESA decided to develop a technology demonstartion mission (SMART-2) as a pre-cursor to test essential technology components and systems in the near future.

Further information: http://www.lisa.uni-hannover.de/, http://lisa.jpl.nasa.gov/, http://sci.esa.int/home/lisa/index.cfm.

9.2 ACES/PHARAO (Atomic Clock Ensemble in Space/Projet d'Horloge Atomique par Refroidissement d'Atomes en Orbite)

Scientific Objectives: (i) To set up the PHARAO clock on the International Space Station and to study its performance in space. (ii) Together with an hydrogen maser to establish a time scale which can be compared with clocks on ground to an accuracy of 10^{-16} which is an anourmous improvement over the present GPS synchronization. Thus an ultra-heigh performance of a global time-synchronization should be achieved which allows new navigation and positioning applications. (iii) To perform

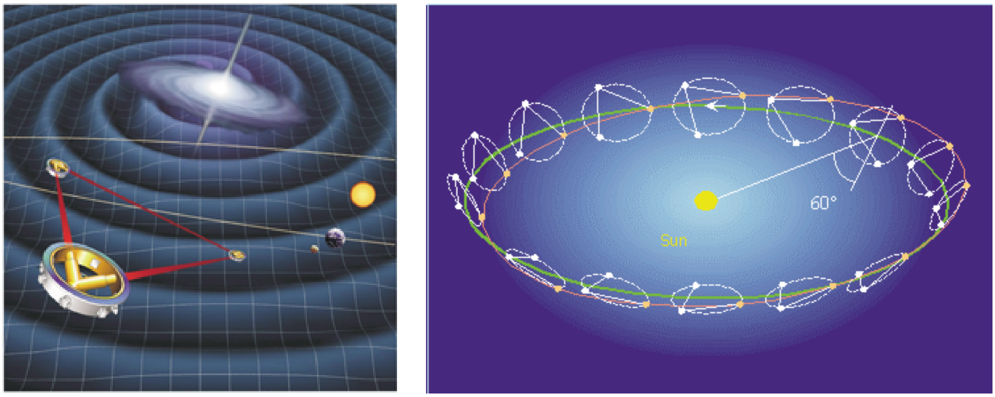

Fig. 8 The detection of gravitational waves. **Left:** An inspiraling binary system creating gravitational waves. **Right:** Formation flight of the three LISA satellites.

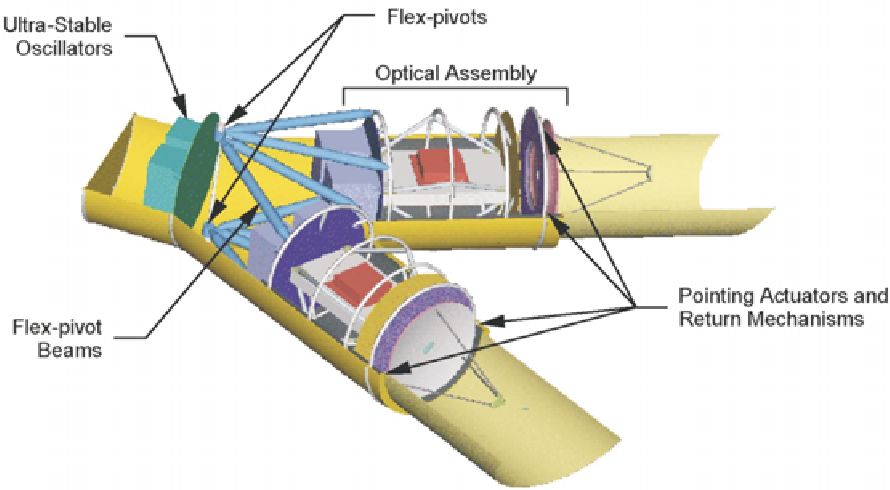

Fig. 9 Payload of one of the three LISA satellites.

tests of the Gravitational Red Shift (improvement by more than one order to present tests) and to search for a time-dependence of the fine structure constant α up to 10^{-16} per year by comparison of the PHARAO with the H-maser clock. (iv) Searching for an anisotropy in the velocity of light to an accuracy of $2 \cdot 10^{-16}$, which is possible since the optical and microwave electromagnetic waves are propagated in different directions when ACES clocks are compared with ground clocks.

Experimental Payload: The payload consists in the PHARAO clock which is a clock based on a fountain of cold Cesium atoms. The scheme of PHARAO is presented in Fig. 10. Additional components are the MWL (MicroWave Link) (replacing the formerly considered optical communication link T2L2 (Time Transfer by Laser Link)) which sends short bursts of light (100 picoseconds) between clocks on Earth and the clocks on the ISS to synchronize them. The payload will be placed on the ISS on an external platform.

Mission Scenario: The MWL operates through sending signals from Earth to the ISS where the arrival time is recorded and where the signal is also reflected to go back to Earth. By means of the signal's round trip it is possible to eliminate fluctuations in the travel time due to the atmosphere. The mission is planned to run for 18 months.

Technology: In this mission for the first time laser cooling techniques and atom traps will be established and tested in space. Furthermore, also for the first time the performance of atom optical elements can be tested in space. All these techniques will be of importance for the HYPER mission, see p. 137. In addition, appropriate microwave links had to be developed.

Further information: `http://opdaf1.obspm.fr/www/pharao.html`, `http://www.cnes.fr/activites/connaissance/physique/1index.htm`

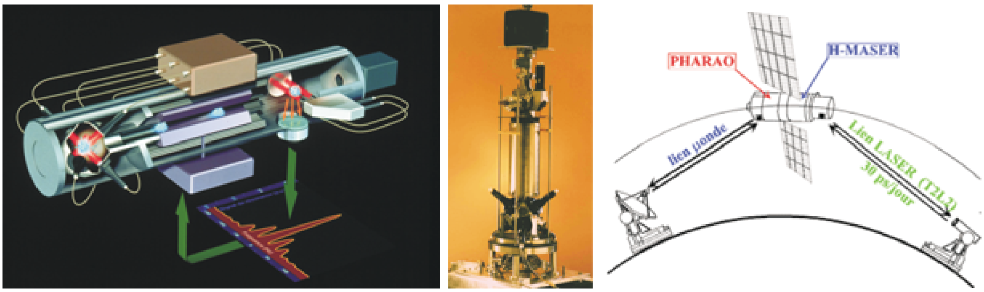

Fig. 10 **Left:** Scheme of the atomic fountain clock PHARAO. Cesium atoms are captured by six lasers and form an optical molasses (left). From this molasses they are released with a velocity of the order of 10 cm/s. They move through a zone of resonant microwave interaction. After the interaction the atoms are in a different state what can be detected by fluorescence. Due to the small velocity the atoms have an interaction time of more than 5 seconds which is more than one order of magnitude longer than it is possible on Earth. **Middle:** The zero-*g* qualified prototype of an atomic clock for space: The cooling zone is at the bottom, the interaction zone in the middle, and the detection zone at the top. The length of the setup is about 1 m. **Right:** The ACES ensemble consisting of the PHARAO and the hydrogen maser clock. Optical and microwave links establish connections to Earth for time and frequency transfer.

9.3 STEP (Satellite Test of the Equivalence Principle)

Scientific Objectives: STEP is, as MICROSCOPE, an experiment to prove the WEP. STEP should be capable of comparing rates of free fall for two test masses of different composition to an accuracy of $\eta \leq 10^{-18}$, where η is the Eötvös factor defined in Eq. (6). The accuracy will be 3 orders of magnitude more precise than that of MICROSCOPE. The difference of STEP compared to MICROSCOPE is (1) the use of SQUID-based sensing technique (a heritage from the Gravity Probe B experiment) for displacement measurements to a very high precision of $7 \cdot 10^{-14}$ in 10^5 s of integration time, and (2) the measurement of the relative motion of the test masses by abandoning the closed loop servo control proposed for MICROSCOPE. Therefore, the drag free control for STEP requires a compensation of disturbing accelerations to less than 10^{-14} m$/(\mathrm{s}^2\sqrt{\mathrm{Hz}})$, never attained in satellite attitude control before.

Experimental Payload: The STEP experiment comprises four differential accelerometers operated simultaneously. Each accelerometer contains two cylindrically symmetric and concentric test masses. Motion along the cylindrical axes are measured with the SQUID magnetometers, motions in radial (perpendicular) direction are hint by superconducting magnetic bearing. In addition, a capacitance sensing and positioning system (similar to the MICROSCOPE system) measures in all degree of freedom at lower resolution and can be used to control and to manipulate the test masses' position actively. It also performs charge estimation and control. The accelerometers are inside a vaccum container and cooled down to a nominal temperature of approximately 2 K in a Dewar with a volume of about 600 l. The test masses are superconductor (Niobium)-coated and face pick-up coils on each side along their symmetric, sensitive axis (see Fig. 11). So, any movement towards a pick-up coil (and away from the other one) changes the inductance values. Because of flux conservation in the superconducting circuit, a small net current through a third (SQUID coupling) coil in parallel with the pick-up coils is forced and can be measured as an inductance signal roughly proportional to the displacement. If both pick-up loops of both test masses are in parallel, a proper set-up enables to measure differential and common displacements simultaneously. The common mode signal is used to control the spacecraft thrusters for drag free control.

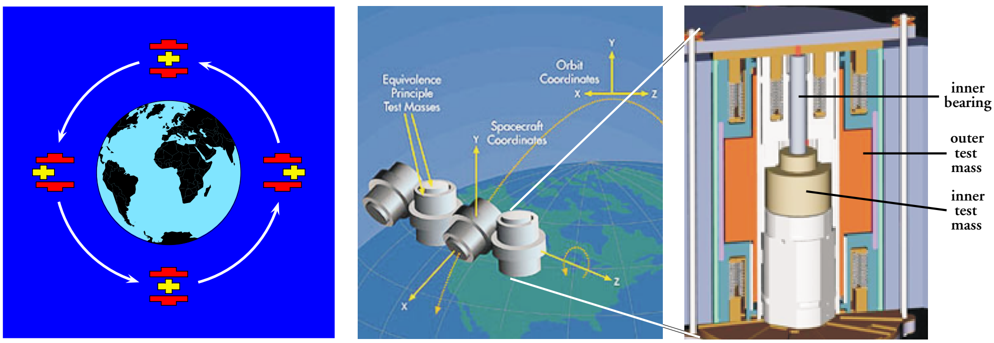

Fig. 11 **Left:** The mission scenario. **Middle:** Orientation of the four pairs of test masses in orbit. **Right:** One pair of test masses and its bearing structure.

The experiment will be carried out with two test mass pairs made from platinum/iridium (Pt/Ir) – niobium (Nb) and Nb – berrylium (Be), as well as with two identical made from Pt/Ir – Be, having a cyclic condition in which the total acceleration difference between the pairs of test masses must add to zero when the WEP holds. The design also incorporates a duplication of one test mass pair for control of systematic, not known failures. The test masses will be fabricated to tolerances smaller than 1 μm. Their shapes and dimensions are optimized to minimize the coupling of higher order gravitational gradients to the individual test masses which reduces spurious effects like helium tides in the Dewar during orbiting the Earth and spacecraft deformations by temperature variations etc.

Mission Scenario: STEP will be launched into a sun-synchronous orbit. The spacecraft faces the sun with its axis perpendicular to the sensitive accelerometer axes. Therefore, the WEP-violation signal can be modulated by spinning the spacecraft. For different spin rates, various analytical in-orbit calibration and signal measurement procedures can be carried out. The ability to shift the signal frequency away from the orbital frequency and any other disturbing frequency is essential for the mission. Many disturbances occur at orbit frequency and its harmonics. Because test masses and spacecraft form a spring-mass-system, the signal frequency is the difference between the reciprocals of orbital time and spin rate. Its phase is such that zero amplitude occurs when the sensitive axis of the accelerometer is horizontal (parallel to the orbit tangent). Data will be taken for intervals of about 20 orbits at spin rates of -3 to $+3$ times orbit frequency. The in-orbit calibration and test phases cover an essential part of the whole mission and aim to test the influences by magnetic bearing forces, gravity gradient, electric charging, temperature variations, satellite motions, magnetic shielding, particle radiation, helium tide, and test mass dynamics by misalignments.

Technology: To test the WEP by six orders of magnitude better than in laboratory where well-established and high performance technology is used, a variety of technological developments had to be made for the STEP mission. Some technologies developed already for GP-B, as the high precision cold gas (Helium proportional) thrusters, the SQUID-based sensing, the Dewar concept for space flight, charge control, and the niobium thin film technique could be applied to STEP with some modifications. Nevertheless, STEP needs a much higher precision level and made it necessary to develop a variety of new technologies. To supress helium tide effects, an aerogel filling of the Dewar is foreseen. Ongoing experimental studies show that the helium II (superfluid helium) liquid-vapour interface does not change shape in response to gravity. The drag-free performance of STEP is 2 orders of magnitude better than for GP-B and 4 orders of magnitude more precise than for MICROSCOPE. This needs much improved modelling of the test mass movements and the spacecraft control loops as well as a precise modelling of thermal, charging, and radiation effects. In addition, test mass fabrication has to be done with very high precision which also needs a high performance metrology. Therefore, STEP will be a challenging mission and a milestone for follow-up missions in fundamental physics not only for experimental techniques but also for spacecraft technology.

Further information: [76], `http://einstein.stanford.edu/STEP/index.html`.

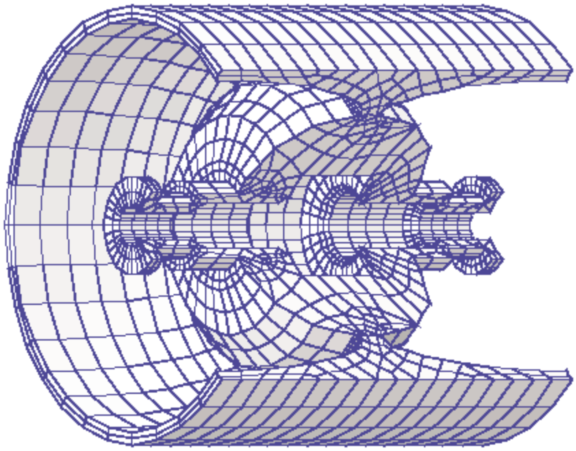

Fig. 12 The microwave cavity for the SUMO mission. Its radius is about 1.3 cm. Due to its special design, this cavity is very robust against microgravity noise (g – jitter).

9.4 SUMO (Superconducting Microwave Oscillator)

Scientific Objectives: Laser cooled atomic clocks with stabilities in the range of 10^{-16} to 10^{-18} coupled with ultrastable superconducting cavity oscillators enable very precise tests of many fundamental laws in gravitation theory. SUMO is an experimental facility developed by the Jet Propulsion Laboratory (JPL), Pasadena CA, and the W.W. Hansen Physics Laboratory of the Stanford University to test (i) the isotropy of space up to $\delta c/c \leq 10^{-18}$, (ii) the independence of the velocity of light from the velocity of the laboratory up to $\delta c/c \leq 3 \cdot 10^{-18}$, and (iii) the universality of the Gravitational Red Shift to $\delta\alpha \leq 10^{-7}$. The first test is a Michelson-Morley experiment to measure the amplitude A of the orientation-dependent term of the light speed given in Eq. (3). The second test is a Kennedy-Thorndike experiment to test the velocity dependence of c represented by the amplitude B, see Eq. (2).

Experimental Payload: The central part of the payload consists of three superconducting microwave cavities mounted orthogonally. The experiments will be carried out on board the International Space Station (ISS) in the Low Temperature Microgravity Physics Facility (LTMPF), a huge liquid helium Dewar allowing access to temperatures down to 0.5 K for durations up to several months.

Mission Scenario: ISS has a low Earth circular orbit with a height of about 350 km and an inclination of about 50°. Therefore the velocity change during one orbit is more than one order larger than on Earth. The gravitational potential differences are small since the ISS is on a nearly circular orbit. A serious problem on the ISS is the high vibration noise in all frequency ranges. Also ISS attitude and orbit control is only rough and results in systematic errors.

Technology: SUMO needed a special development of superconducting cavity oscillators with ultrastable behaviour. The essential improvement compared to all measurements on Earth will be due to the high thermostability and the low level of residual acceleration acting on the experiment in a weightlessness environment.

The approached levels of stability are $\delta_{\rm acc}\nu/\nu \sim 6.5 \cdot 10^{-9}$ per g, and $\delta_T\nu/\nu \sim 3 \cdot 10^{-10}$ per degree Kelvin. The robustness against gravitational accelerations comes from a special design of the cavities, see Fig. 12. Temperature stability is achieved by means of cryogenic temperatures.

Further information: [13, 14], `http://bigben.stanford.edu/sumo/`.

9.5 STM (SpaceTime Mission)

Scientific Objectives: (i) Searching for a violation of the universality of the Gravitational Red Shift at the 10^{-10} level with three different trapped ion clocks clocks based on mercury, cadmium, and ytterbium (which are different in their electromagnetic composition) possessing a stability of 10^{-16} in about $7 \cdot 10^4$ s and which approach the Sun to within four Solar radii. (ii) Search for spatial and temporal variations of the fine structure constant increasing present estimates by 6 orders of magnitude. The deep space trajectory of this mission is optimized for making $\Delta U/c^2$ as big as possible. Fig. 13 shows the mission szenario. A Jupiter gravity assigned fly-by maneuver enable to increase $\Delta U/c^2$ to $5.3 \cdot 10^{-7}$, which is the best value obtainable in the solar system.

Experimental Payload: The main part of the payload consists of the three ion clocks (Fig. 14) based on the trapped ion frequency standards of the JPL (for a description of ion clocks see, e.g., [99]). The main advantages of the present setup consists of (i) all traps share the same vacuum chamber applied potentials, magnetic and thermal environment, (ii) use of a single local oscillator from which all three hyperfine signals can be derived. The experimental arrangement implies that that most environmental perturbations and noises will be common to the ions confined in the three traps. Furthermore, ambient magnetic fields can be eliminated by using one of the ions as a probe of these fields.

Mission Scenario: After launch the spacecraft will be injected towards Jupiter which will redirect the motion of the spacecraft towards the Sun which should be passed by at a distance of $(4.2 \pm 0.2)\, R_\odot$. Spacecraft navigation is no problem. At closest solar approach the external temperature of about 2000 K will be shielded

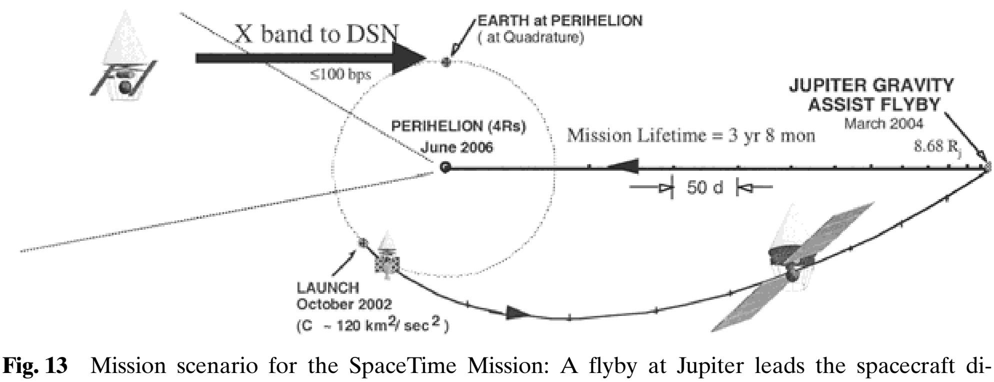

Fig. 13 Mission scenario for the SpaceTime Mission: A flyby at Jupiter leads the spacecraft directly to the sun.

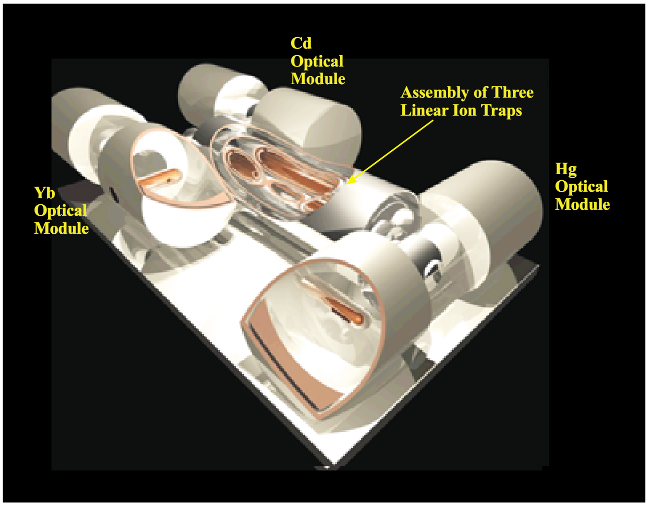

Fig. 14 The Tri-Clock Ensemble for the SpaceTime Mission consisting of clocks based on trapped mercury, cadmium and ytterbium.

by a conical solar blocking element, IR shields, High Temperature Multi Layer Insulation, and support structure to give inside the spacecraft an operation temperature of about 0 to 40 °C.

Technology: For the clocks the technology of JPL frequency standards is used. The temperature shields are under development.

Further information: [77].

9.6 HYPER (HYPER precision atom interferometry in space)

Scientific Objectives: This missions aims (i) to measure the Lense-Thirring effect in a way which is somehow complementary to the GP-B mission. While GP-B averages the gravitomagnetic field over the whole orbit, in HYPER, due to the possibility to read out the atomic interference pattern on a short timescale, it is possible to scan the spatial distribution of the gravitomagnetic field $\nabla \times \boldsymbol{h}$. (ii) In addition, a better value for the fine structure constant α can be obtained by atom

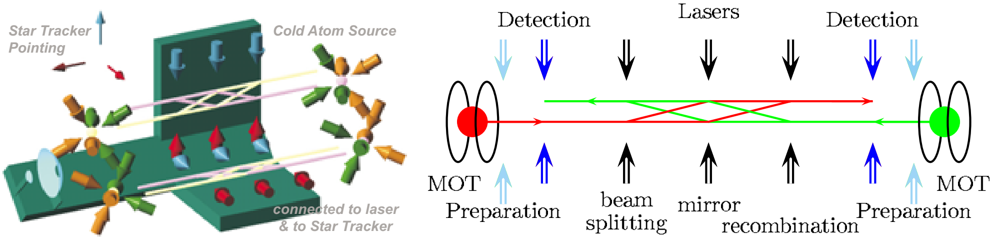

Fig. 15 **Left:** The central part of the HYPER payload, the ASU (Atomic Sagnac Unit), consists of an optical bench, lasers, the atomic source and a telescope. **Right:** Scheme of the two atom interferometers of the ASU. After being cooled in a MOT the atoms are prepared with a drift velocity and then split by three subsequently $\pi/2$, π, and $\pi/2$ laser beams. Behind the recombination is the detection area.

interferometry in space. (iii) By means of atom interferometry it is possible to perform a test of the WEP with *quantum matter* to the order of 10^{-15}. (iv) By observing the visibility of the interference fringes an estimate on a hypothetical fundamental decoherence, as it may be induced by space-time fluctuations, can be given, (v) to establish atom interferometry as high precision inertial sensor for accelerations and rotations rates.

Experimental Payload: The essential part of this mission is the ASU (Atomic Sagnac Unit) which consists of two orthogonal pairs of atom interferometers in a Ramsey-Bordé configuration based on cesium and/or rubidium together with an atom source and a magneto-optical trap (MOT) for cooling and storing the atoms. The atomic beam splitting as well as the cooling and detection of the interfering atoms after leaving the interferometer is carried through with lasers. All optical devices have to be mounted on an optical bench which is rigidly connected with a star tracking telescope pointing very precisely on the chosen guide star.

Mission Scenario: In orbit, the ASU first traps about 10^9 atoms in a vapour cell in the MOT and cools them down to less than 100 μK. By means of a sub-Doppler cooling method they can be further cooled down to a few μK. Applying an adjusted laser frequency, the atoms are accelerated to their final drift velocity and prepared in appropriate electronic states which are insensitive to magnetic stray fields. After that the the atomic beams are split and recombined by means of three counter-propagating laser beams which is the actual interferometer. In order to improve the sensitivity, two interferometers with atoms propagating in opposite directions are implemented.

Technology: The technological feasibility of this mission is under study at ESA. Many of the atom optical elements (lasers, MOT, optical bench) have already been proven space-qualified since they will be used in the PHARAO project.

Further information: [36].

9.7 ASTROD (Astrodynamical Space Test of Relativity using Optical Devices)

Scientific Objectives: In a single mission the following experiments should be carried through: (i) High-precision measurement of relativistic effects (especially the PPN parameters β and γ) with 3 to 6 orders of magnitude improvement, (ii) measurement of solar angular momentum via the Lense-Thirring effect, (iii) determination of the solar g-modes by means of measuring the Sun's gravitational field, (iv) improvement in the measurement of G and of its time derivative $\dot{G}$, (v) the detection of low-frequency gravitational waves in the range of 50 μHz to 5 mHz, (vi) better determination of orbits and masses of planets and major asteroids, and (vii) exploration of an constant anomalous acceleration towards the Sun.

Experimental Payload: The basic ASTROD concept consists of two spacecrafts in solar orbits each having as payload (i) a drag-free system with a proof mass, accelerometers with a noise level of 10^{-13} to $3 \cdot 10^{-15}$ m/($s^2 \sqrt{\text{Hz}}$) from 50 μHz to 5 mHz and an absolute stability of 10^{-13} to 10^{-15} m/s^2, and FEEPs, (ii) two 1 to 2 W lasers stabilized to 10^{-15} as they are developed for LISA, (iii) two telescopes, again as developed for LISA, and (iv) a light-weight clock with a precision better

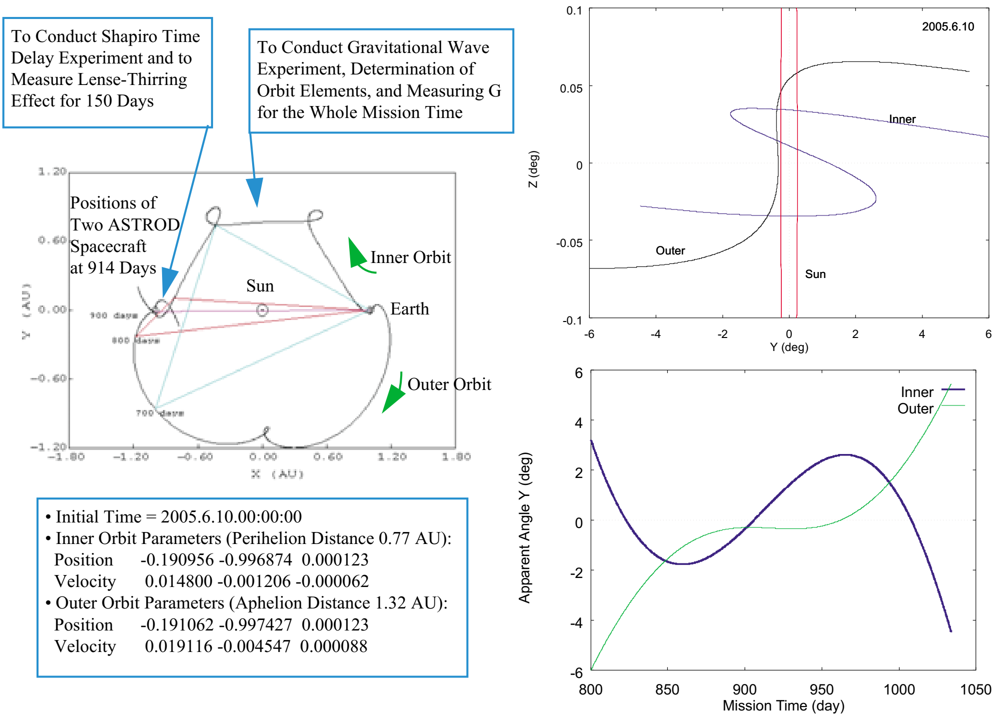

Fig. 16 **Left:** The inner and outer orbits of the two ASTROD spacecrafts in the Sun-Earth fixed frame. **Top right:** The apparent angles of the two ASTROD spacecrafts located respectively on the inner and outer orbits near two and half years after launch. **Bottom right:** Apparant angle Y vs. mission time.

than 10^{-15}. The two spacecraft communicate with the Earth reference system during the whole mission, and communicate with each other when they are near.

Mission Scenario: Observation of the two drag-free spacecrafts, one beeing in an outer, and the other in an inner solar orbit (Fig. 16). The ranging times between Earth reference system and the two spacecrafts are monitored through the whole mission. The ranging times between the two spacecrafts are monitored when they are near each other around 2.5 years and 7.5 years after launch to measure the solar angular momentum via Lense-Thirring effect. From fitting the ranging data to the corresponding theoretical model, the quantities described in the scientific objectives can be read off.

Technology: Most challenging for this mission may be the development of optical technology to carry out laser interferometry over 2 AU. Research and development have been started recently.

Further information: [19, 86, 135].

9.8 WEAX (Weak Equivalence Antiproton eXperiment)

Scientific Objectives: Testing the Weak Equivalence Principle for antimatter with 10^{-3} accuracy on ISS using the LTMPF.

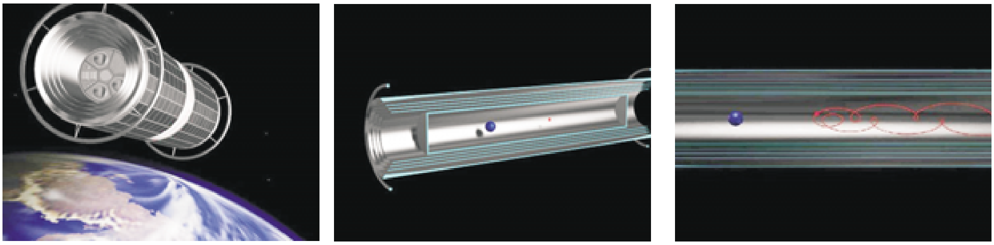

Fig. 17 The SEE satellite, cutaway view and particle trajectories.

Experimental Payload: The apparatus where the whole experiment is included consists of three traps which during the mission should be integrated into the LTMPF of the ISS. First, there is a storage trap, then a cooling and transfer trap and at last the weighting trap where the positrons fulfill their specific dynamics which is sensitive to the gravitational acceleration.

Mission Scenario: Around 10^4 antiprotons before the mission produced on Earth will be stored in a Penning trap at about 2 K. In orbit, before the actual experiment, these antiprotons will be cooled down to 0.1 μeV and piccenice injected into the so-called "weighting trap" where they fulfill a gravitationally modified magnetron motion which can be measured. – The main limitations of this setup are due to the microgravity environment of the ISS, the small size of the experiment and the resolution of the detector.

Technology: Since the production of positrons has been demonstrated in particle accelerators (compare the ATHENA-project at CERN), and since the transportation and storage of particles and thus of anti-particles for a long time of the order of years is no problem, all the technology required for this mission exist and is shown to work. The space-qualification of these technologies remains to be demonstrated.

Further information: [58].

9.9 SEE (Satellite Energy Exchange)

Scientific Objectives: The main objectives of this mission are (i) to test the gravitational inverse square law at the separation of meters (provided by test masses inside the satellite) and of the radius of the Earth, (ii) to test the WEP, (iii) to search for a time variation of the gravitational constant G, (iv) to determine the value of the gravitational constant G, and (v) to search for an anisotropy of space.

Experimental Payload: The satellite consists of a big cylindrical vacuum tube, within which are two or more free-floating test masses (Fig. 17). In order to track freely falling masses inside the satellite, an optical ranging system belongs to the payload.

Mission Scenario: The satellite has to be placed in a Sun-synchronous orbit which is important for stable temperature conditions. From the calculated paths of the test masses it is necessary that the symmetry axes of the satellite always is tangential to the orbital path. During the mission a large test mass (the "Shepherd") is free-floating continuosly for the duration of the mission (several years), and one or more small test masses are launched inside the satellite and their trajectories relative to the Shepherd are observed. From the observed trajectories consequences about the above objectives can be drawn.

Technology: The essential part of the mission is the ranging of free falling masses inside the satellite below micrometers. Therefore, a new method for distance measurements, MAARS (Micron Accuracy Absolute Ranging System), has been developed. This system is based on Fresnel diffraction and is capable of determinig absolute distances (rather than relative distances) with sub-micron precision at distances exceeding one meter. Because one knows the absolute distance it is not necessary to track the test masses continuously which reduces errors due to radiation pressure.

Further information: [103–106], `http://gravity.phys.utk.edu/see/`

9.10 OPTIS (Optical Test of the Isotropy of Space)

Scientific Objectives: (i) Test of the isotropy of light propagation (Michelson-Morley experiment) up to the order of $\delta c/c \leq 10^{-18}$, (ii) test of the independence of the speed of light from the velocity of the laboratory to the order of $\delta_v c/c \leq 10^{-16}$, and (iii) test of the equality of the Gravitational Red Shift for an atomic clock and an optical clock to the order 10^{-4}.

Experimental Payload: This consists of a monolithic crossed resonator, two ultra-stable Nd : YAG lasers, an atomic clock and an optical comb generator, see Fig. 18. The advantage of the monolithic resonator is that fluctuations in the temperature influence both resonators in the same way so that this leads to no errors for the Michelson-Morley experiment.

Mission Scenario: A compromise with respect to the orbit has to be found. For Kennedy-Thorndike tests, a low eccentric orbit with no ecclipse phases would be ideal, whereas for Michelson-Morley tests a high orbit would be preferred. Furthermore, also charging during crossing the van-Allen belt must be avoided with respect to the reference sensor. Therefore, a high elliptical orbit with its peregree at 10,000 km and its apogee at 40,000 km has been chosen. In a first phase,

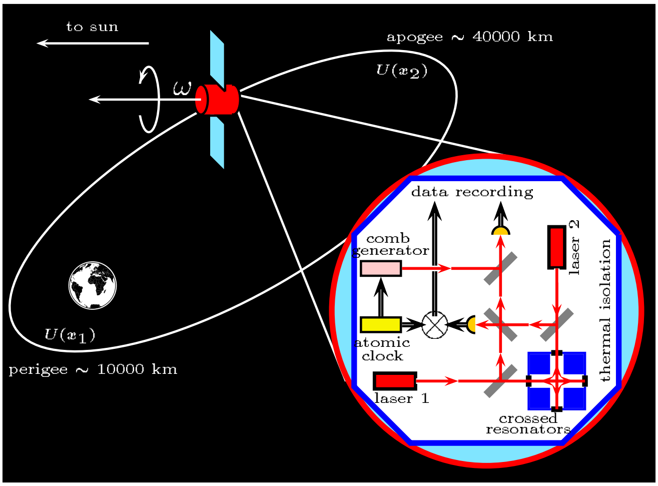

Fig. 18 Scheme of OPTIS: The science payload of the satellite mainly consists of two crossed resonators to which two lasers are locked, an atomic clock and an optical comb generator. The orbit of the satellite is highly elliptic.

the satellite will be flawn in a Geo Transfer Orbit. After carrying out the Kennedy-Thorndike test, the satellite will be transferred to a highly eccentric orbit by means of a kick-motor. For such an orbit the environment is very quite which is of advantage for the Michelson-Morley experiment. In addition, the potential difference is large and, therefore ideal for the universality of red shift experiment.

Technology: For the OPTIS-mission ultrastable monolithic resonators have to be developed and used. The lasers are ultrastable Nd:YAG laser which are already space-proven. In order to perform the Kennedy-Thorndike test and the tests of the universality of the Gravitational Red Shift, an additional time standard is needed for which an atomic clock based on cesium or rubidium will be taken. In order to be able to make a comparison of the resonator frequency and the frequency of the atomic clock to the required accuracy, a newly invented device, the optical frequency comb [30], will be used. This new technology is very important for future metrology experiments, especially in space. As far as the satellite bus and the orbit is concerned, capacative sensors and FEEPs will be used to perform drag-free attitude and orbit control.

Further information: [69].

9.11 GG (Galileo Galilei)

Scientific Objectives: GG is an idea to launch a small satellite in low Earth orbit to test the WEP to 10^{-17} with rotating test masses. The basic idea of the experiment is that a high frequency modulation of the WEP-violating signal occuring with orbit frequency can improve the signal to noise ratio and that high frequency rotation reduces influences by temperature, dissipation, and thermal noise. If the test masses have cylindrical shape and rotate perpendicularly to the orbital plane (see Fig. 19), any WEP-violation would cause an oscillation of the centres of mass.

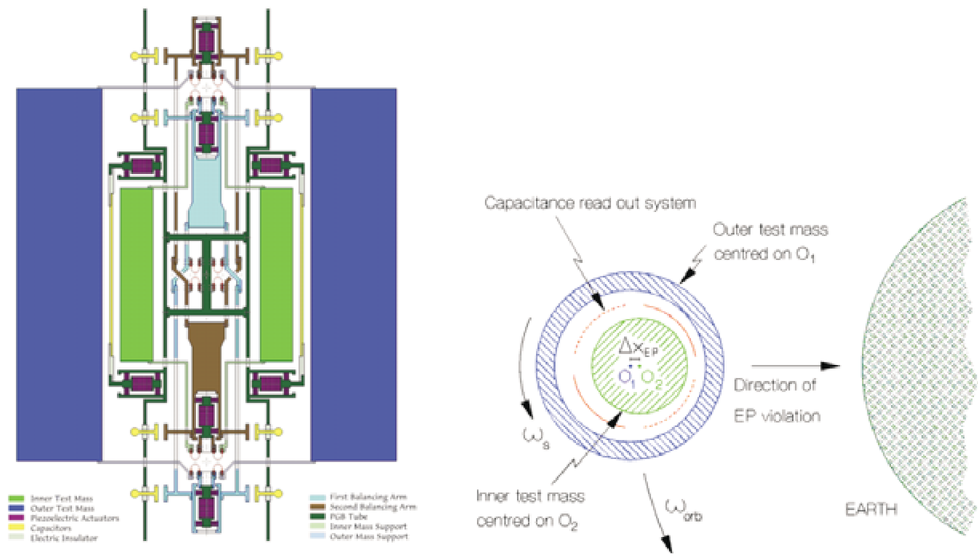

Fig. 19 **Left:** Schematic view of the GG satellite. **Right:** Schematic view of the GG mission.

The spin rate of the satellite is 5 Hz. The crucial experimental problem is to make the mechanical coupling weak enough to sense a possible deviation from Newtonian mechanics. The sensor would detect a signal of the form

$$\delta x = \delta x_{\text{WEP}} \cos\left(\omega_{\text{spin}} t + \phi_{\text{WEP}}\right) x_F \,, \tag{26}$$

where δ_x is the relative displacement caused by an eventual, ω_{spin} is the spacecraft spin, ϕ_{WEP} is the phase of the WEP-violating signal, and $x_F = \cos\theta + \sin\theta\cos\left(\omega_{\text{orbital}} t + \phi\right)$ is a geometrical term depending on the orbit frequency ω_{orbital} and the angle θ between spin axis and orbit normal.

Experimental Payload: The two test masses are hollow cylinders of 10 kg mass placed concentrically and rotated around their symmetry axis which itself is aligned with the spacecraft spin axis. The test masses are made from different materials. The suspensions must be carefully clamped to avoid mechanical losses. The experiment is run at room temperature. The spacecraft spin must be stabilized but does not need active attitude control. Nevertheless drag compensation must be provided by use of ion thrusters. The experiment can be flown in any circular orbit. Test mass oscillations are measured by means of a capacitance read-out system.

Mission Scenario: Despite mechanical problems to attain high precision, there are reasons to consider the GG-experiment: (1) a very high modulation frequency of the signal, to be achieved easily by passive one-axis stabilization of the spacecraft, (2) the absence of all major electric charging effects, provided for free by the mechanical suspensions, which seems to be the most challenging problem, (3) to be carried out at room temperature.

Technology: The experiment needs very good mechanical suspension systems with small internal dissipation as these suspensions undergo minute deformations at the spin frequency. The suspension system guarantees the very weak coupling required for the high precision WEP test. A ground version GGG (Galileo Galilei on the Ground) is under development.

Further information: `http://tycho.dm.unipi.it/nobili`.

10 Summary and Outlook

As a summary one may confront all the scientific objectives of space missions with the actually proposed space missions. The result can be seen in Fig. 20.

It can be taken from this Figure that there are several classes of missions which are defined by means of their scientific payload and/or of their scientific objectives:

(i) Tests of SR and the universality of the Gravitational Red Shift. Since these tests have to be carried out with clocks, the corresponding missions rely on the development and the use use of high precision clocks. Since atomic clocks are rather stable against accelerations, missions using these clocks are not relying strongly on drag-free control. Clocks based on resonators, for example, need very stable drag-free control. However, in this case this is no scientific necessity but merely the realization of a quiet environment which is needed for the resonators.

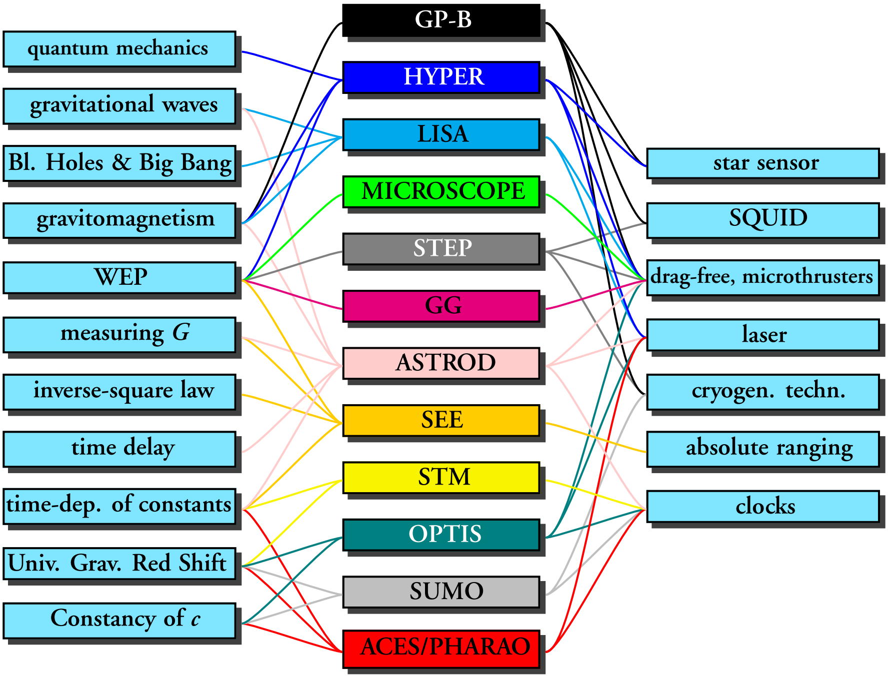

Fig. 20 List of scientific objectives, the corresponding projects, and the various techniques for space missions.

(ii) Regarding the scientific objectives, beside the SR test most missions test the WEP. This is understandable because this kind of tests clearly use the space conditions (long time of free fall) and because this topic is well motivated by theoretical predictions.

(iii) Another objective of many missions is the Lense-Thirring effect. However, while GP-B and HYPER, for example, try to verify this effect, it will be used by other missions in order to determine the angular momentum of the Sun.

Other scientific objectives, like the test of the inverse square law and test of quantum mechanics are connected with single missions only which, however, additionally aim to reach further research goals.

The drag-free control and the microthrusters, e.g., FEEPs, are a very important experimental tool for many space missions. These devices are needed either for technical reasons (deformation-free components) or for a geodetic motion which is needed for the corresponding experiments as, for example, for the tests of the WEP or of the Lense-Thirring effect. Another universal tool are lasers which either serve as part of a Doppler tracking system or as part for the specific experimental setup as, e.g., in HYPER. Contrary to that, the star sensor (telescope), SQUID and cryogenic techniques are rather mission specific developments needed for the mission to test the Lense-Thirring effect and for measuring the relative accelerations in WEP tests.

From this scheme it is also clear in which way the technological developments may be streamlined: the development of clocks, lasers, and drag-free control are devices which are used by most of the missions. On the scientific side one cannot draw a general conclusion like that because each mission is important by itself.

As we told in the introduction, space projects for FP become more and more popular due to the space conditions which in most cases are really of big advantage in order to considerably improve the experimental results. This is reflected by the fact that there are more and more proposals for fundamental physics in space. Not always it is necessary to have one's own satellite for a space mission. In some cases also an experiment if carried out on the ISS (like PHARAO/ACES, SUE, BEST, SUMO, and WEAX) may give a huge improvement of physical results, even though on Space Station a certain level of mechanical noise (g-jitter) is unavoidable. In any case space conditions are in many cases mandatory in order to achieve progress in experimental physics.

The authors are indebted to Ch. Bordé, K. Danzmann, V. Dohm, W. Ertmer, C. F. W. Everitt, F. Hehl, Th. Konrad, J. Lipa, N. Lockerbie, L. Maleki, J. Mester, W.-T. Ni, A. Nobili, E. Rasel, Ch. Salomon, A. Sanders, G. Schäfer, S. Schiller, T. Sumner, P. Touboul, S. Vitale for a lot of discussions and help. We especially like to thank all the members of the ESA Topical Team on Fundamental Physics on the ISS (see http://www.uni-duesseldorf.de/TT) for their contributions.

References

[1] Fundamental physics in space roadmap. NASA, JPL 1999, `http://funphysics.jpl.nasa.gov/technical/library/roadmap.html`

[2] J. Alfaro, H. A. Morales-Tecotl, and L. F. Urrutia, L., Quantum gravity corrections to neutrino propagation. Phys. Rev. Lett. **84** (2000) 2318

[3] G. Amelino-Camelia, G. Ellis, N. E. Mavromatos, D. V. Nanopopulos, and S. Sarkar, Tests of quantum gravity from observations of gamma-ray bursts. Nature **393** (1998) 763

[4] S. D. Biller et al., Limits to quantum gravity effects on energy dependence of the speed of light from observations of TeV flares in active galaxies. Phys. Rev. Lett. **83** (1999) 2108

[5] C. J. Bordé, Atomic interferometry with internal state labeling. Phys. Lett. A **140** (1989) 10

[6] C. J. Bordé, Theoretical tools for atom optics and interferometry. C. R. Acad. Sci. Paris Série IV 2 (2001) 509

[7] C. J. Bordé, J.-C. Houard, and A. Karasievich, Relativistic phase shifts for Dirac particles interacting with weak gravitational fields in matter-wave interferometers. In: *Gyros, Clocks, and Interferometers: Testing Relativistic Gravity in Space*, C. Lämmerzahl, C. W. F. Everitt, and F. W. Hehl, Eds. Lecture Notes in Physics vol. 562, Springer-Verlag, Berlin, 2001, p. 403

[8] M. Born and L. Infeld, Foundations of the new field theory. Proc. R. Soc. London A **144** (1934) 425

[9] D. Bowmeester, A. Ekert, and A. Zeilinger, Eds., The Physics of Quantum Information. Springer Verlag, Berlin, 2000

[10] A. Brillet and J. L. Hall, Improved laser test of the isotropy of space. Phys. Rev. Lett. **42** (1979) 549

[11] H. N. Brown et al. (Muon ($g-2$) Collaboration), Precise measurement of the positive Muon anomalous magnetic moment. Phys. Rev. Lett. **86** (2001) 2227

[12] Č. Bruckner, M. Żukowski, and A. Zeilinger, The essence of entanglement. quant-ph/0106119

[13] S. Buchman, M. Dong, S. Wang, J. A. Lipa, and J. P. Turneaure, A space-based superconducting microwave oscillator clock. Adv. Space Res. **25** (2000) 1251

[14] S. Buchman, J. Turneaure, J. Lipa, M. Dong, K. Cumbernack, and S. Wang, A superconducting microwave oscillator clock for use on the space station. Proceedings of the IEEE International Frequency Symposium IEEE (1998) 534

[15] R. Burke et al., Positron production in multiphoton light-by-light scattering. Phys. Rev. Lett. **79** (1997) 1626
[16] P. Busch, P. J. Lahti, and P. Mittelstaedt, The Quantum Theory of Measurement. Springer-Verlag, Berlin, 1991
[17] S. M. Carroll, G. B. Field, and R. Jackiw, Limits on Lorentz- and parity-violating modifications of electrodynamics. Phys. Rev. D **41** (1990) 1231
[18] Y. T. Chen and A. Cook, Gravitational Experiments in the Laboratory. Cambridge University Press, Cambridge, 1993
[19] D.-W. Chiou and W.-T. Ni, ASTROD Orbit Simulation and Accuracy of Relativistic Parameter Determination. Adv. Space Res. **25** (2000) 1259
[20] T. C. P. Chui and W.-T. Ni, Experimental search for an anomalous spin-spin interaction between electrons. Phys. Rev. Lett. **71** (1993) 3247
[21] T. E. Chupp, R. J. Hoara, R. A. Loveman, E. R. Oteiza, J. M. Richardson, and M. E. Wagshul, Results of a new test of local Lorentz invariance: A search for mass anisotropy in ^{21}Ne. Phys. Rev. Lett. **63** (1989) 1541
[22] I. Ciufolini, The 1995–99 measurements of the Lense-Thirring effect with using laser-ranged satellites. Class. Quantum Grav **17** (2000) 2369
[23] I. Ciufolini, F. Chieppa, D. Luccesi, and F. Vespe, Test of Lense-Thirring orbital effect due to spin. Class. Quantum Grav. **14** (1997) 2701
[24] I. Ciufolini, E. Pavlis, F. Chieppa, E. Fernandes-Vieira, and J. Pérez-Mercader, Test of General Relativity and measurement of the Lense–Thirring effect with two Earth satellites. Science **279** (1998) 2100
[25] I. Ciufolini and J. A. Wheeler, Gravitation and Inertia. Princeton University Press, Princeton, 1995
[26] T. Damour and A. M. Polyakov, The string dilaton and a least action principle. Nucl. Physics B **423** (1994) 532
[27] T. Damour and A. M. Polyakov, String theory and gravity. Gen. Rel. Grav. **12** (1996) 1171
[28] T. W. Darling, F. Rossi, G. I. Opat, and G. F. Moorhead, The fall of charged particles under gravity: A study of experimental problems. Rev. Mod. Phys. **64** (1992) 237
[29] Ch. Daussy, T. Marrel, A. Amy-Klein, C. T. Nguyen, C. T. Bordé, and C. Chardonnet, Limit on the parity nonconserving energy difference between the enantiomers of a chiral molecule by laser spectroscopy. Phys. Rev. Lett. **83** (1999) 1554
[30] S. A. Diddams et al., Direct link between microwave and optical frequencies with a 300 THz femtosecond laser comb. Phys. Rev. Lett. **84** (2000) 5102
[31] R. W. P. Drever, A search for the anisotropy of inertial mass using a free precession technique. Phil. Mag. **6** (1961) 683
[32] J. Ellis, S. Hagelin, D. V. Nanopoulos, and M. Srednicki, Search for violations of quantum mechanics. Nucl. Phys. B **241** (1984) 381
[33] J. Ellis, N. E. Mavromatos, and D. V. Nanopoulos, Probing models of quantum space–time foam. gr-qc/9909085
[34] J. Ellis, N. E. Mavromatos, D. V. Nanopoulos, and G. Volkov, Gravitational–recoil effects on fermion propagation in space-time foam. gr-qc/9911055
[35] W. Ertmer, E. M. Rasel et al., Atom interferometry and optics in space — a European programme for fundamental physics on the ISS. Final report of the ESA Topical Team, ESA 2001 (forthcoming)
[36] W. Ertmer et al., HYPER — Hyper–precision cold atom interferometry in space; Assessment study report. ESA, Noordvijk, 2000
[37] T. M. Eubanks, D. N. Matsakis, J. O. Martin, B. A. Archinal, D. A. McCarthy, S. A. Klioner, S. Shapiro, and I. I. Shapiro, Advances in solar system tests of gravity. Talk at the 1997 ARR Meeting of the APS, http://flux.aps.org/meetings/YR97/BAPSAPR97/abs/S1280005.html
[38] C. W. F. Everitt, S. Buchman, D. B. DeBra, G. M. Keiser, J. M. Lockhart, B. Muhlfelder, B. W. Parkinson, J. P. Turneaure, and other members of the Gravity Probe B team. Gravity Probe B: Countdown to launch. In: *Gyros, Clocks, and Interferometers: Testing Relativistic*

Gravity in Space, C. Lämmerzahl, C. W. F. Everitt, and F. W. Hehl, Eds. Lecture Notes in Physics vol. 562. Springer-Verlag, Berlin, 2001, p. 52

[39] J. L. Feng and K. T. Matchev, Supersymmetry and the anomalous magnetic moment of the Muon. Phys. Rev. Lett. **86** (2001) 3480

[40] E. Fischbach and C. L. Talmadge, The Search for Non-Newtonian Gravity. Springer-Verlag, New York, 1999

[41] M. E. Fisher, Renormalization group theory: Its basis and formulation in statistical physics. Rev. Mod. Phys. **70** (1998) 653

[42] L. H. Ford and N. F. Svaiter, Focusing vacuum fluctuations. Phys. Rev. A **62** (2000) 062105

[43] B. Frois and M.-A. Bouchiat, Eds. Parity Violation in atoms and Polarized Electron Scattering (Singapore, 1999), World Scientific

[44] R. Gambini and J. Pullin, Nonstandard optics from quantum space-time. Phys. Rev. D **59** (1999) 124021

[45] A. S. Goldhaber and M. M. Nieto, Terrestrial and extraterrestrial limits on the photon mass. Rev. Mod. Phys. **43** (1971) 277

[46] P. T. Greenland, Antimatter. Contemp. Phys. **38** (1997) 181

[47] K. Greisen, End of the cosmic ray spectrum? Phys. Rev. Lett. **16** (1966) 748

[48] R. Grieser, R. Klein, G. Huber, S. Dickopf, I. Klaft, P. Knobloch, P. Merz, F. Albrecht, M. Grieser, D. Habs, D. Schwalm, and T. Kühl, A test of special relativity with stored lithium ions. Appl. Phys. B **59** (1994) 127

[49] T. L. Gustavson, A. Landragin, and M. A. Kasevich, Rotation sensing with a dual atom–interferometer sagnac gyroscope. Class. Quantum Grav. **17** (2000) 2385

[50] N. D. Hari Dass, Test for C, P, and T nonconservation in gravitaton. Phys. Rev. Lett. **36** (1976) 393

[51] N. D. Hari Dass, Experimental tests for some quantum effects in gravitation. Ann. Physics (N.Y.) **107** (1977) 337

[52] M. P. Haugan, Energy conservation and the principle of equivalence. Ann. Phys. **118** (1979) 156

[53] M. P. Haugan and T. F. Kauffmann, A new test of the Einstein equivalence principle and the isotropy of space. Phys. Rev. D **52** (1995) 3168

[54] W. Heisenberg and H. Euler, Folgerungen aus der Diracschen Theorie des Positrons. Z. Physik. **98** (1936) 714

[55] D. Hils and J. L. Hall, Improved Kennedy–Thorndike experiment to test special relativity. Phys. Rev. Lett. **64** (1990) 1697

[56] C. D. Hoyle, U. Schmidt, B. R. Heckel, E. G. Adelberger, J. H. Gundlach, D. J. Kapner, and H. E. Swanson, Submillimeter test of the gravitational inverse–square law: A search for large extra dimensions. Phys. Rev. Lett. **86** (2001) 1418

[57] C.-H. Hsieh, P.-Y. Jen, K.-L. Ko, K.-Y. Li, W.-T. Ni, S.-S. Pan, Y.-H. Shih, and R.-J. Tyan, The equivalence principle experiment for spin–polarized bodies. Mod. Phys. Lett. **4** (1989) 1597

[58] F. M. Huber, R. A. Lewis, E. W. Messerschmid, and G. A. Smith, Precision tests of Einstein's weak equivalence principle for antimatter. Adv. Space Res. **25** (2000) 1245

[59] F. M. Huber, E. W. Messerschmidt, and G. A. Smith, The WEAX-experiment. Class. Quantum Grav. **18** (2001) 2457

[60] M. C. E. Huber, M. Jacob, and B. Battrick, Eds., Fundamental Physics in Space & Related Topics, Convenor's Summaries of the ESA-CERN Workshop 5-7 April 2000. ESA Publication Division, ESTEC Noordwijk, 2001

[61] R. J. Hughes, The equivalence principle. Contemp. Phys. **34** (1993) 177

[62] V. W. Hughes, H. G. Robinson, and V. Beltran-Lopez, Upper limit for the anisotropy of inertial mass from nuclear resonance experiments. Phys. Rev. Lett. **4** (1960) 342

[63] C. J. Isham, Lectures on Quantum Theory. Imperial College Press, London, 1995

[64] R. J. Kennedy and E. M. Thorndike, Experimental establishment of the relativity of time. Phys. Rev. **42** (1932) 400

[65] D. Krause and E. Fischbach, Searching for extra dimensions and new string-inspired forces in the Casimir regime. In: *Gyroscopes, Clock, Interferometers, …: Testing Relativistic Gravity in*

Space, C. Lämmerzahl, C. W. F. Everitt, and F. W. Hehl, Eds. Lecture Note in Physics vol. 562. Springer-Verlag, Berlin, 2001, p. 292

[66] C. Lämmerzahl, Quantum tests of Lense-Thirring type effects. To appear in the Proceedings of the 3rd Fairbanks Meeting, Rome 1998

[67] C. Lämmerzahl, Quantum tests of foundations of general relativity. Class. Quantum Grav. **14** (1998) 13

[68] C. Lämmerzahl, On the experimental foundation of the Maxwell equations. In: *Recent Developments on Exact Solutions and Scalar Fields in Gravity*, A. Macias, J. Cervantes, and C. Lämmerzahl, Eds. Kluver Academic / Plenum Publishers, New York, 2001, p. 295

[69] C. Lämmerzahl, H. Dittus, A. Peters, and S. Schiller, OPTIS – a satellite based test of special and general relativity. Class. Quantum Grav. **18** (2001) 2499

[70] C. Lämmerzahl, C. W. F. Everitt, and F. W. Hehl, Eds. Gyros, Clocks, Interferometers . . .: Testing Relativistic Gravity in Space (Berlin, 2001), Lecture Notes in Physics vol. 562, Springer-Verlag

[71] C. Lämmerzahl and M. P. Haugan, On the interpretation of Michelson-Morley experiments. Phys. Lett. A **282** (2001) 223

[72] C. Lämmerzahl and G. Neugebauer, The Lense-Thrring effect: From the basic notions to the observed effects. In: *Gyroscopes, Clock, Interferometers, . . .: Testing Relativistic Gravity in Space*, C. Lämmerzahl, C. W. F. Everitt, and F. W. Hehl, Eds. Lecture Notes in Physics vol. 562. Springer-Verlag, Berlin, 2001, p. 31

[73] S. K. Lamoreaux, Demonstration of the Casimir force in the 0.6 to 6 μm range. Phys. Rev. Lett. **78** (1997) 5

[74] S. K. Lamoreaux, J. P. Jacobs, B. R. Heckel, F. J. Raab, and E. N. Fortson, New limits on spatial anisotropy from optically pumped ^{201}Hg and ^{199}Hg. Phys. Rev. Lett. **57** (1986) 3125

[75] J. Leitner and S. Okubo, Parity, charge conjugation, and time reversal in the gravitational interaction. Phys. Rev. B **136** (1964) 1542

[76] N. Lockerbie, J. C. Mester, R. Torii, S. Vitale, and P. W. Worden, STEP: A status report. In Gyros, Clocks, and Interferometers: Testing Relativistic Gravity in Space, C. Lämmerzahl, C. W. F. Everitt, and F. W. Hehl, Eds. Lecture Notes in Physics vol. 562. Springer-Verlag, Berlin, 2001, p. 213

[77] L. Maleki and J. Prestage, SpaceTime mission: Clock test of relativity at four solar radii. In: *Gyros, Clocks, and Interferometers: Testing Relativistic Gravity in Space*, C. Lämmerzahl, C. W. F. Everitt, and F. W. Hehl, Eds. Lecture Notes in Physics vol. 562. Springer-Verlag, Berlin, 2001, p. 369

[78] R. Mansouri and R. U. Sexl, A test theory of special relativity: I. Simultaneity and clock synchronisation. Gen. Rel. Grav. **8** (1977) 497

[79] R. Mansouri and R. U. Sexl, A test theory of special relativity: II. First order tests. Gen. Rel. Grav. **8** (1977) 515

[80] R. Mansouri and R. U. Sexl, A test theory of special relativity: III. Second order tests. Gen. Rel. Grav. **8** (1977) 809

[81] C. W. Misner, K. Thorne, and J. A. Wheeler, Gravitation. Freeman, San Francisco, 1973

[82] E. W. Morley and D. C. Miller (letter to Lord Kelvin). Phil. Mag. **8** (1904) 753

[83] E. W. Morley and D. C. Miller, Report of an experiment to detect the FitzGerald-Lorentz-effect. Phil. Mag. **9** (1905) 680

[84] W.-T. Ni, A nonmetric theory of gravity. Preprint http://gravity5.phys.nthu.edu.tw (1973) Montana State University, Bozeman, Montana, USA

[85] W.-T. Ni, Equivalence principles and electromagnetism. Phys. Rev. Lett. **38** (1977) 301

[86] W.-T. Ni, Testing relativistic gravity and measuring solar system parameters vio optical space mission. In: *Gyros, Clocks, and Interferometers: Testing Relativistic Gravity in Space*, C. Lämmerzahl, C. W. F. Everitt, and F. W. Hehl, Eds. Lecture Notes in Physics vol. 562. Springer-Verlag, Berlin, 2001, p. 330

[87] M. M. Nieto and T. Goldman, The arguments against "antigravity" and the gravitational acceleration of antimatter. Phys. Rep. **205** (1991) 222

[88] K. Nordtvedt, Lunar laser ranging – a comprehensive probe of the post-newtonian long range interaction. In: *Gyroscopes, Clock, Interferometers, . . .: Testing Relativistic Gravity in Space*,

C. Lämmerzahl, C. W. F. Everitt, and F. W. Hehl, Eds. Lecture Notes in Physics vol. 562. Springer-Verlag, Berlin, 2001, p. 317
[89] L. B. Okun', Test of electric charge conservation and the Pauli principle. Usp. Fiz. Nauk. **158** (1989) 293
[90] K. Pennicott, Muons threaten the Standard Model. Physics World **14** (March 2001), 3
[91] I. C. Percival, Atom interferometry, spacetime and reality. Physics Today **10** (1997) 43
[92] A. Peres, Test of the equivalence principle with spin. Phys. Rev. D **18** (1978) 2739
[93] A. Peters, K. Y. Chung, and S. Chu, Measurement of gravitational acceleration by dropping atoms. Nature **400** (1999) 849
[94] J. D. Prestage, J. J. Bollinger, W. M. Itano, and D. J. Wineland, Limits for spatial anisotropy by use of nuclear-spin-polarized $^9Be^+$ ions. Phys. Rev. Lett. **54** (1985) 2387
[95] J. D. Prestage, R. L. Tjoelker, and L. Maleki, Atomic clocks and variations of the fine structure constant. Phys. Rev. Lett. **74** (1995) 3511
[96] R. J. Protheroe and H. Meyer, An infrared background-TeV gamma-ray crisis? Phys. Lett. B **493** (2000) 1
[97] N. F. Ramsey, Electric dipole tests of time reversal symmetry. American Institute of Physics Conference Proceedings **323** (1995) 3
[98] R. D. Reasenberg, I. I. Shapiro, P. E. MacNeil, R. B. Goldstein, J. C. Breidenthal, J. P. Brenkle, D. L. Cain, T. M. Kaufman, T. A. Komarek, and A. I. Zygielbaum, Viking relativity experiment: verification of signal retardation by solar gravity. Astrophys. J. Lett. **234** (1979) L219
[99] F. Riehle, Clocks for length and time measurement. In: *Gyros, Clocks, and Interferometers: Testing Relativistic Gravity in Space*, C. Lämmerzahl, C. W. F. Everitt, and F. W. Hehl, Eds. Lecture Notes in Physics vol. 562. Springer-Verlag, Berlin, 2001, p. 347
[100] R. C. Ritter, L. I. Winkler, and G. T. Gillies, Search for anomalous spin-dependent forces with a polarized-mass torsion pendulum. Phys. Rev. Lett. **70** (1993) 701
[101] H. P. Robertson, Postulate versus observation in the Special Theory of Relativity. Rev. Mod. Phys. **21** (1949) 378
[102] A. Roy, C.-Y. Lin, and U. Mohideen, Improved precision measurement of the Casimir force. Phys. Rev. D **60** (1999) 111101
[103] A. J. Sanders, A. D. Alexeev, S. W. Allison, V. Antonov, K. A. Bronnikov, J. W. Campbell, M. R. Cates, T. A Corcovilos, D. D Earl, T. Gadfort, G. T. Gillies, M. J. Harris, N. I. Kolosnitsyn, M. Yu. Konstantinov, V. N. Melnikov, R. J. Newby, R. G. Schunk, and L. L. Smalley, Project SEE (Satellite Energy Exchange): an international effort to develop a space-based mission for precise measurements of gravitation. Class. Quantum Grav. **17** (2000) 2331
[104] A. J. Sanders, A. D. Alexeev, S. W. Allison, K. A. Bronnikov, J. W. Campbell, M. R. Cates, T. A. Corcovilos, D. D. Earl, T. Gadfort, G. T. Gillies, M. J. Harris, N. I Kolosnitsyn, M. Yu. Konstantinov, V. N. Melnikov, R. J. Newby, R. G. Schunk, and L. L. Smalley, Project SEE (Satellite Energy Exchange): proposal for space-based gravitational measurements. Meas. Sci. Technol. **10** (1999) 514
[105] A. J. Sanders and W. E. Deeds, Proposed new determination of the gravitational constant G and tests of Newtonian gravitation. Phys. Rev. D **46** (1992) 489
[106] A. J. Sanders and G. T. Gillies, A comparative survey of proposals for space-based determination of the gravitational constant G. Revista Nuovo Cim. **19** (1996) 1
[107] B. E. Schaefer, Severe limits on variations of the speed of light with frequency. Phys. Rev. Lett. **82** (1999) 4964
[108] G. Schäfer, Testing general relativity. Adv. Space Res. **25** (2000) 1115
[109] S. Schiller, Proposed test of the time independence of the fundamental constants α and m_e/m_p using monolithic resonators. Phys. Rev. D **64** (2001) to appear
[110] M. Schneider, J. Müller, U. Schreiber, and D. Egger, Hochpräzisionsvermessung der Mondbewegung. Astronomie und Raumfahrt **34** (1997) 4
[111] J. Schwinger, On gauge invariance and vacuum polarization. Phys. Rev. **82** (1951) 664
[112] S. Seel, R. Storz, G. Ruoso, J. Mlynek, and S. Schiller, Cryogenic optical resonators: A new tool for laser frequency stabilization at the 1 Hz level. Phys. Rev. Lett. **78** (1997) 4741
[113] I. I. Shapiro, Fourth test of general relativity. Phys. Rev. Lett. **13** (1964) 789

[114] I. I. Shapiro, Solar system tests of General Relativity: recent results and present plans. In: *General Relativity and Gravitation*, N. Ashby, D. Bartlett, and W. Wyss, Eds. Cambridge University Press, Cambridge, 1990, p. 313

[115] A. Shimony, Proposed neutron interferometer test of some nonlinear variants of wave mechanics. Phys. Rev. A **20** (1979) 394

[116] C. G. Shull, D. K. Atwood, J. Arthur, and M. A. Horne, Search for a nonlinear variant of the Schrödinger equation by neutron interferometry. Phys. Rev. Lett. **44** (1980) 765

[117] C. G. Shull, K. W. Billmann, and F. A. Wedgwood, Experimental limit for the neutron charge. Phys. Rev. **153** (1967) 1415

[118] M. H. Soffel and J. Müller, Lasermessungen der Monddistanz. Sterne und Weltraum **7** (1997) 646

[119] R. I. Steinberg, K. Kwiatkowski, W. Maenhaut, and N. S. Wall, Experimental test of charge conservation and the stability of the electron. Phys. Rev. D **12** (1975) 2582

[120] R. W. Stover, T. I. Moran, and J. W. Trischka, Search for an electron-proton inequality by charge measurements on an isolated macroscopic body. Phys. Rev. **164** (1967) 1599

[121] Y. Su, B. R. Heckel, E. G. Adelberger, J. H. Gundlach, M. Harris, G. L. Smith, and H. E. Swanson, New test of the universality of free fall. Phys. Rev. D **50** (1994) 3614

[122] T. J. Sumner, Fundamental physics in space – UK scientific aims and opportunities in future. Community Report to PPARC Space Science Advisory Committee, 2000

[123] H. Thirring and J. Lense, Über den Einfluß der Eigenrotation der Zentralkörper auf die Bewegung der Planeten und Monde nach der Einsteinschen Gravitationstheorie. Phys. Z. **19** (1918) 156

[124] K. S. Thorne, D. L. Lee, and A. P. Lightman, Foundations for a theory of gravitation theories. Phys. Rev. D **7** (1973) 3563

[125] P. Touboul, Space accelerometers: Present status. In: *Gyroscopes, Clock, Interferometers, ...: Testing Relativistic Gravity in Space*, C. Lämmerzahl, C. W. F. Everitt, and F. W. Hehl, Eds., Lecture Notes in Physics vol. 562. Springer-Verlag, Berlin, 2001, p. 274

[126] B. J. Venema, P. K. Majumder, S. K. Lamoreaux, B. R. Heckel, and E. N. Fortson, Search for a coupling of the Earth's gravitational field to nuclear spin in atomic mercury. Phys. Rev. Lett. **68** (1992) 135

[127] R. F. C. Vessot and M. V. Levine, A test of the equivalence principle using a space-borne clock. Gen. Rel. Grav. **10** (1979) 181

[128] R. F. C. Vessot, M. V. Levine, E. M. Mattison, E. L. Blomberg, T. E. Hoffmann, G. U. Nystrom, B. F. Farrel, R. Decher, P. B. Eby, C. R. Baughter, J. W. Watts, D. L. Teuber, and F. D. Wills, Test of relativistic gravitation with a space-borne hydrogen maser. Phys. Rev. Lett. **45** (1980) 2081

[129] W. Vodel, H. Dittus, S. Nietzsche, H. Koch, J. Zameck Glyscinski, R. Neubert, S. Lochmann, C. Mehls, and D. Lockowandt, High sensitive DC SQUID-based position detectors for application in gravitational experiments at the drop tower Bremen. In: *Gyroscopes, Clock, Interferometers, ...: Testing Relativistic Gravity in Space*, C. Lämmerzahl, C. W. F. Everitt, and F. W. Hehl, Eds. Lecture Notes in Physics vol. 562. Springer-Verlag, Berlin, 2001, p. 248

[130] J. K. Webb, M. T. Murphy, V. V. Flambaum, V. A. Dzuba, J. D. Barrow, C. W. Churchill, J. X. Prochaska, and A. M. Wolfe, Further evidence for cosmological evolution of the fine structure constant. Phys. Rev. Lett. **87** (2001) 091301

[131] C. M. Will, Theory and Experiment in Gravitational Physics (Revised Edition). Cambridge University Press, Cambridge, 1993

[132] J. G. Williams, X. X. Newhall, and J. O. Dickey, Relativity parameters determined from lunar laser ranging. Phys. Rev. **53** (1996) 6730

[133] D. J. Wineland, J. J. Bollinger, D. J. Heinzen, W. M. Itano, and M. G. Raizen, Search for anomalous spin-dependent forces using stored-ion spectroscopy. Phys. Rev. Lett. **67** (1991) 1735

[134] F. C. Witteborn and W. M. Fairbank, Experimental comparison of the graviational force on freely falling electrons and metallic electrons. Phys. Rev. Lett. **19** (1967) 1049

[135] A.-M. Wu, X. Xu, and W.-T. Ni, Orbit design and analysis for the ASTROD mission concept. Int. J. Mod. Phys. D **9** (2000) 201

[136] G. T. Zatsepin and V. A. Kuzmin, Upper limit of the spectrum of cosmic rays. JETP Lett. **4** (1966) 78.